UNIVERSITY OF DEBRECEN
FACULTY OF ENGINEERING
DEPARTMENT OF
MECHANICAL ENGINEERING

INTEGRATED FINITE ELEMENT ANALYSIS OF A GENERATIVE DESIGNED PROSTHETIC HIP STEM FOR ADVANCED MANUFACTURING

MASTER'S THESIS

KHALEEL ABDULLAH OMAR ALKHATEIB
Production Engineering Specialization

Debrecen
2026

Table of Contents

Introduction

In medical application rapid manufacturing, engineering challenges are really important to be addressed, as it impacts human life directly and it requires golden standard for any medical device designed to be surgically used for implantation. It is important also to ensure the safety and the long life of the prosthesis as well as comfort and proper function that would ultimately determine the patients' quality of life.

As additive manufacturing is embedded more and more, with the potential of being fully integrated into the medical field, the paradigm is projected to shift from conventional manufacturing to mass customization with rapid manufacturing, which creates the ability to not just modify the size of the piece around the discrete sizing standards but also to tailor the part to the specific needs and the quality of the bone in case of the patient based on the health, age, or the bone regeneration rate for the bones around the implant. As the possibility for integration of 3D printers in local hospitals becomes more possible, and the logistics costs potentially being illuminated, it is more feasible to create medical devices that are mass customized in the hospital.

This thesis note addresses the benefits of Rapid Prototyping and Rapid Manufacturing, with the experimentation involving also the concept of generative design, which is also known as the topology optimization to simplify and improve the geometrical shape of a custom hip implant, to discover a creative solution that will if successful; significantly improve the current implementation strategy. In hopes of creating a solution that can be beneficial for more than the 5 million humans per year worldwide that are in need of this surgery, as well as to benefit future researchers and create a roadmap for young students in this field.

1 Literature Review

In order to understand the evolution of technology and the fundamentals of how the modern Hip Arthroplasty has implemented and leveraged advanced manufacturing techniques in order to produce patient specific solutions. Advances in Additive Manufacturing technology are discussed that revolutionized the fields of rapid prototyping, as well as the field of rapid manufacturing, which has been significant over the past 40 years.

1.1 Anatomy and Clinical Context

The surgical integration for the intervention to restore the function of the joint, and relieve the pain for patients that are suffering from the severe degeneration of joints has been very and highly successful, it is known as Total Hip Arthroplasty (THA), the most apparent indication for osteoarthritis in the application of THA in hip replacement surgery is the progressive deterioration of the articular cartilage In the underlying bone in the femoral head [13].

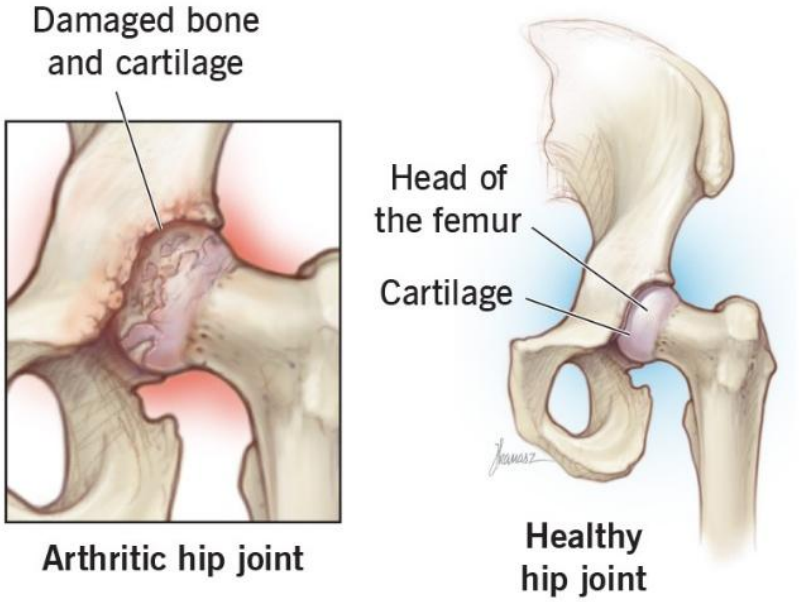

Figure 1.1. Degeneration at the femoral head [13].

That degenerative disease that is illustrated in the picture above is called osteoarthritis (Hip arthritis), osteoarthritis is the leading cause for 90% of the hip implant replacement arthroplasty worldwide, which is the degeneration of the femoral head, and this typically requires the hip implant procedure with replacing

not only the femur but also the acetabular socket [12]. As the cartilage continues to wear bone on born friction result and leads to severe pain and restricted mobility as well as high stiffness [12].

The hip implant is not just a one component system, but a multi component system that is typically made from the acetabular cup and the ceramic liner laying on top of it as well as the femoral head and the femoral stem [16].

Figure 1.2. Modular and Monoblock hip implants [16].

The femoral stem has evolved from more than the monoblock design where the them and they had were single component, to the current state-of-the-art modular design, the modularity allows the customization of the join offset and the length of the leg my independently selecting the stems and the heads during the design process before the procedure [16].

While the hip implant is composed from three parts and the main one is the femoral head which is connected directly to the bones and fixated with the bones [14]. It is also important to realize the fixation technique for the stem which is the main focus on the design and manufacturing in this thesis.

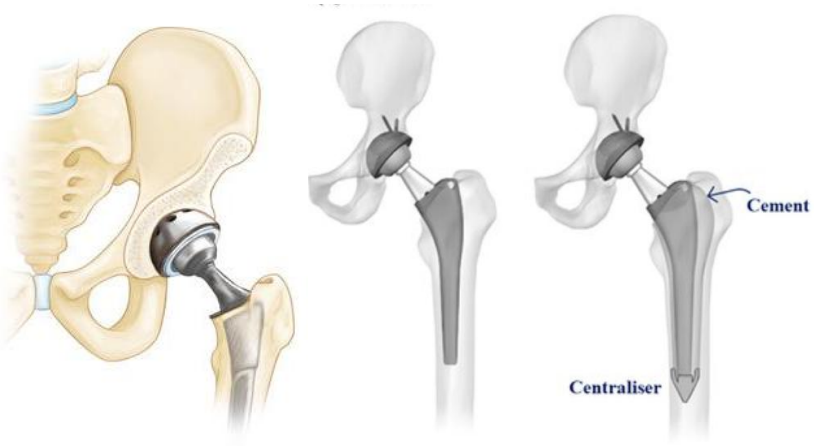

Figure 1.3. The implant as Fitting into the hip with Cementless and Cemented Fixation [13][14].

Two main principles of fixation are used in THA practice the cemented and the cementless techniques of fixation, are explained as follows:

1. Cemented Fixation uses PMMA bone cement to help anchor the stem part of the hip implant with the femur bone, it can also be used to fix the femoral head [14]. But to focus mainly on the stem fixation, the cemented fixation is used to fill the gaps between the bone and the stem to allow for better load distribution and reduce the chance of a femoral fracture after the hip implant operation [14]. Which is mainly used in older patients that have poor quality bones, where the bone build regeneration around the implantation is also weak [14].

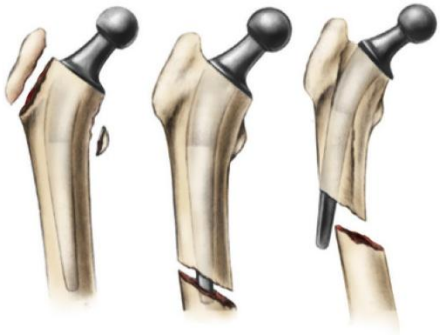

Figure 1.4. The bone around the implant breaking in different ways [12].

2. Cementless Fixation on the other hand is taking advantage of regeneration of the bone tissues around the features of the stem of the hip implant, which are classified as in-growth or on-growth on the interface [14]. This technique is only possible when the quality of the bone can handle the pressing of the stem into the femur without developing fracture, and also when the regeneration or the bone tissue is possible, which is better in younger and more active healthy patients [14].

1.2 Clinical Viability

The main objective for using the manufacturing technology of 3D printing in case of titanium or other material that might be discovered in the future; is to have the ability to introduce structures that are otherwise not possible with conventional manufacturing methods like CNC and casting [15]. Some of these features can be the production of generative design structures as well as inner channels or inner structures fillings and lattice structures that are on the surface which comes to the importance that will be elaborated specifically further [17].

The reason for implementing lattice structure is not just because it creates impossible features to be produced by conventional manufacturing method or because it is a mechanical novelty, but it's also important for the mitigation of phenomenon that causes a lot of biomechanical clinical viability concerns [17].

Clinical viability will be studied in this thesis around 2 main mechanical and biomechanical phenomena, which are stress shielding and the promotion of osseointegration [17].

Very important concept to follow in case of stress shielding, to understand the behavior of the bone, is by the scientist Julius Wolff, the German anatomist surgeon who developed the concept of Wolff's law, which states that healthy bone can adapt to the loads over time that are placed on specific areas of the bone which does not only affect the cortical bone but can also affect the cancellous bone, by helping to increase the density of the bone in the areas where it has Increased physical activity and the bones becoming weaker in areas that are deprived from mechanical stimulation that is required to maintain the bone density [18].

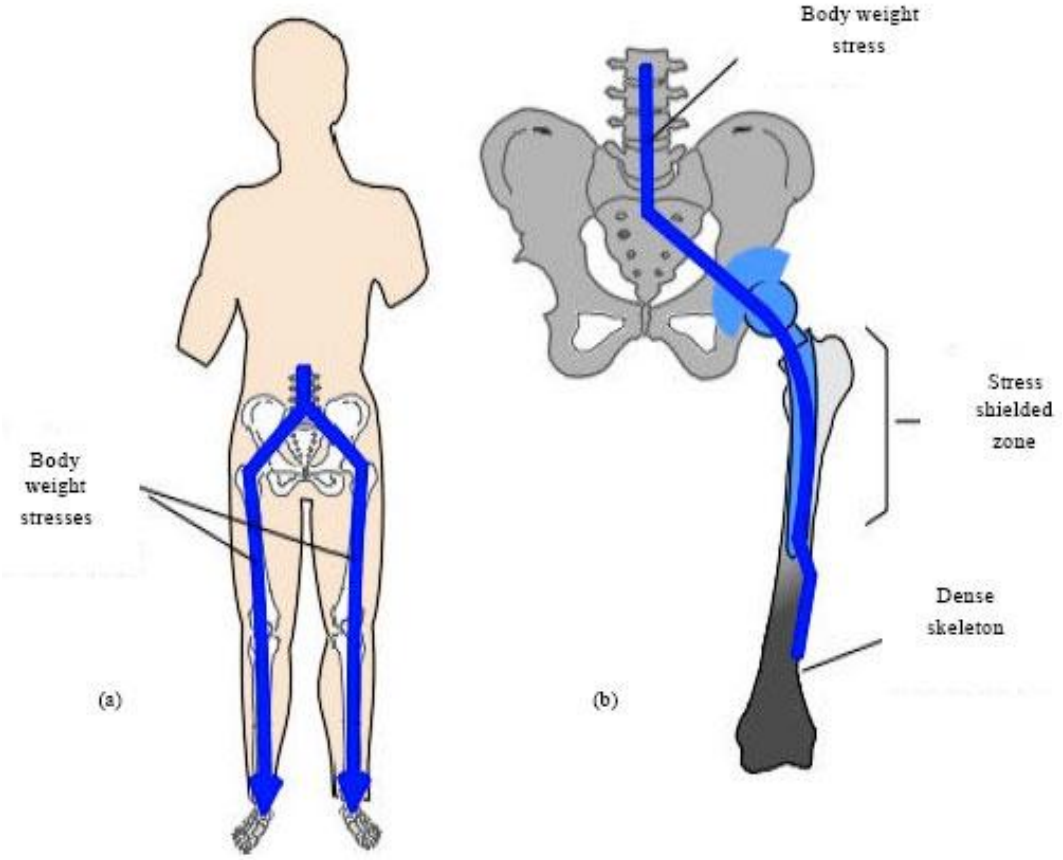

Figure 1.5. Stress Shielding Weight Distribution Scheme [22].

As illustrated in this figure above, the mechanical loads that the hip implant bears are not distributed evenly on the surrounding bone tissue, which creates stress shielded zone that overtime loses the density of the bone in surrounding areas, which in return creates the potential problem of loosening the implant, with severe pain to the patient than as if it was ideally connected through the even weight distribution [22].

1.3 Biomechanics: Stress Shielding & Wolff's law

Despite the initial success of fixation techniques in THA procedures, surrounding bone tissues in relationship with the stem material; has exhibited a biomechanical mismatch, which is caused by the usage of standard solid metal stems, which led to difference in stiffness that caused severe problems and concerns clinically, it is defined in the phenomena of stress shielding [17].

Before explaining stress shielding phenomenal; it is important to understand the ground rule of the dynamic nature for the bone tissues in human bodies as it is explained by Wolff's Law, By the German anatomist wolf in the 19th century, which states that: The bone tissue will adapt and remodel itself overtime in order to accommodate the mechanical loads that are it is being subject to it [18].

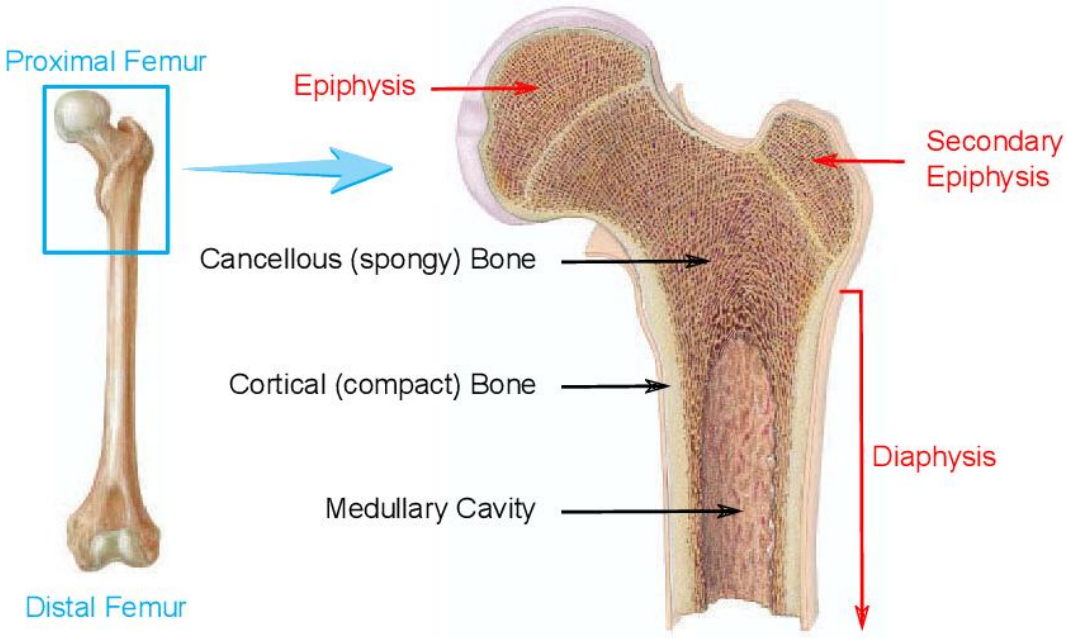

Figure 1.6. Adult human proximal femur cross-section [20].

If the mechanical load increases; the bone well adapt and remodel itself in order to become denser and stronger (hypertrophy), in order to accommodate the sort of mechanical loading, and on the other hand, if the mechanical load decreases, the bone will become less dense and weaker (atrophy), due to the too high metabolic cost of keeping and maintaining bone mass that is unnecessary [18].

When a highly stiff solid metallic stem is inserted into the kernel of the femur which is called the medullary canal, the physiological load distribution is drastically altered from its natural form due to the fact that metals stems are significantly stiffer than the counselors and cortical bone tissues, which can be directly observed as a mismatch, so the implant in this case absorbs the majority of the mechanical loads during the activities of walking or standing which effectively "shields" the surrounding hosting bones from the naturally required mechanical stimulation [17]. Based on the statement of Wolff's law, this lack of mechanical stimulation can overtime trigger bone resorption severely around the implant (osteolysis), Which

eventually leads overtime to the loss of bone density, and in case of cementless fixation, the implant will start loosening, severe pain will be caused to the patient, with the eventual need for a surgery in order to repair the complex effects [18].

In order to prevent the phenomenon of stress shielding which is the main primary biomechanical objective that is focused on by the design of modern hip implants, and to prevent the bone resorption the stiffness of the femoral stem must be controlled and reduced in order to as closely as possible exhibit the same behavior in connection with the natural bone tissues stiffness, as engineers has sought solutions historically in trying to avoid this stiffness mismatch, by the careful selection of biomaterial in orthopedic science [13].

However, there are further differences that can allow the relationship between the femoral stem and the surrounding bone tissues to be in harmony which does not require the changing of the material but the surrounding structure of the femoral stem to accommodate the bone ingrowth over the implant in order to distribute the mechanical loads evenly and not deprive the surrounding bone tissues from the mechanical stimulation that it needs in order to stay dense and healthy [20].

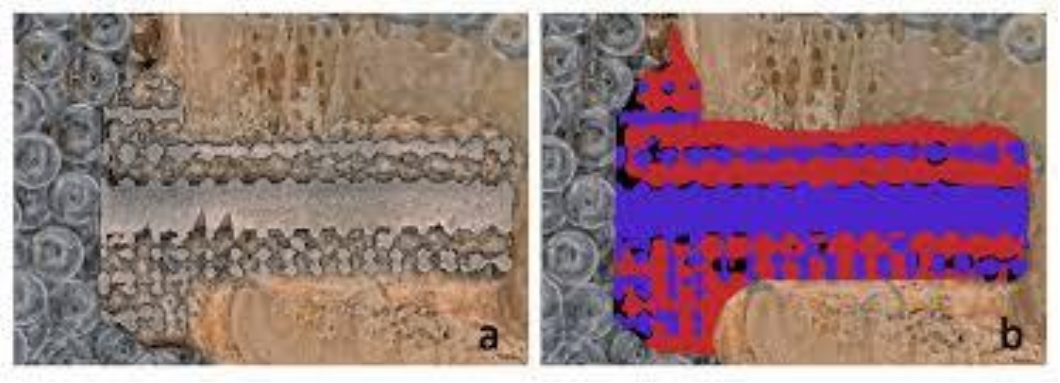

Figure 1.7. Bone In-growth [21].

The direction of the research That was carried on bye A. Kovacs and S. Mano of using lattice structure is different from the aim for this thesis which is the one that uses generative design capabilities, but it's also important to know that in both cases the manufacturing technique is similar as these structures are impossible to be produced by conventional CNC machining even if it has the 5 axis or 6 axis capabilities [21].

However for further future research, It is possible to introduce the generative designed femoral stem and combine it with the lattice structure in order to achieve the possibility of the reduction of stress shielding phenomenon as well as the implementation of the promotion of osseointegration, The usage of classes structure has the potential of solving both of these issues, we'll be careful selection of the lattice structure that has also an enormous effect on the quality of the relationship between the surrounding bone tissues and the femoral stem structures that are in a way the direct communication interface with the natural bone tissues [21].

1.4 Biomaterials in Orthopedic Surgeries

The selection of the material is not just important from the cost factor, but is also reflected on by longevity, as well as some specific needs and constraints that can be attributed to every patient, based on the age, activity level, the quality of the bone in the femoral stem region, as well as the fixation technique [13].

The material selection is dictated by high clinical requirements for that the material must exhibit excellent biocompatibility in order to prevent any autoimmune responses, rejection or toxicity [13]. Mechanical strength in order to endure high mechanical dynamic and static loading can also be tested for fatigue failure, which is important to resist the cats and endure continuous dynamic and static loading cycles without fatigue or fracture, and the ability to resist corrosion in the harsh environment of human bodily fluids which is considered corrosive [12].

Stainless steel 316L has been historically used for femoral stems due to its low cost, is it provided enough strength and the long term clinical performance was not the best as it's still corroded inside the really corrosive environment of human bodily fluids, as well as causing further issues with fatigue failure under continuous cycle which made it an option that is no longer available for the modern THA practice

Table 1.1. Hip-Implant Materials [14].

Material	THA	Cost	Advantages	Limitations
Ti–6Al–4V (titanium alloy)	Femoral stems, porous/lattice coatings	High: depending on alloy and pores processing	Good biocompatibility: relatively low elastic modulus → reduced stress shielding; good fatigue resistance and corrosion resistance.	Lower wear resistance at articulating surfaces; usually not used as bearing couple.
Co–Cr–Mo alloy	Femoral heads, some stems, metal cups	Medium: Raw material cost is low, polishing and finishing are high	High strength and hardness; wear resistance, corrosion resistance.	Higher stiffness: greater risk of stress shielding in the femur.
Stainless steel (e.g. 316L)	Older stems, trauma implants	Low	Good strength, easy to process and relatively low cost.	Inferior corrosion and fatigue performance.
Alumina / zirconia ceramics	Femoral heads, ceramic liners	High: requires advanced manufacturing and quality control.	Excellent wear resistance, very low friction; highly biocompatible.	Vulnerable to edge chips and micro cracks;

Cobalt-Chromium-Molybdenum (Co-Cr-Mo) alloys, the selection for THA femoral head and some stems or metal cups has been the choice for orthopedic industry, in order to improve the long term reliability as well as due to the fact that Co-Cr-Mo exhibited exceptional hardness, as well as an ultra-high tensile strength that can outstand a huge amount of wear and fatigue which made it the choice for articulating components [13]. However, due to the fact that utilizing Co-Cr-Mo for femoral stems makes a lot of biomechanical disadvantages it is important to understand that the human cortical bone Young's modulus is approximately between 15 to 30 GPa, and the Co-Cr-Mo alloys have high Young's modulus of 210 to 240 GPa [14]. The main disadvantage for this material to be used is that it does not evenly distribute the physiological loads on the human bone tissues, which in turn makes the stress shielding phenomenon more prone to happen with bone resorption too [14]. And lastly, the modular taper that is the meeting point between the femoral head and the titanium stem junction, becomes more prone to fretting and corrosion [14].

Titanium alloy and specifically Ti-6Al-4V (Titanium-6Aluminum-4Vanadium) was introduced into the medical field application as it directly addresses the mismatch of the Young's modulus and in order to mitigate the stress shielding, which later became the standard for femoral stems that does not rely on cement for fixation, as it provides balance between the biological properties and the mechanical properties, as well as the advantage of that it forms a stable self-healing dioxide on its surface so it does not becomes susceptible to corrosion and has far superior biocompatibility in comparison with Co-Cr-Mo alloys, with its Young's modulus being half of it at 110 to 114 GPa [13]. It remains stiffer than the natural bone tissues but as it is a point in the middle compared to Co-Cr-Mo alloys, the selection for material is only half the solution and the introduction of the lattice structure is the other half of the solution in order to resolve the issue of biocompatibility [17].

1.5 Additive Manufacturing in Medicine

The first quick prototyping system was patented and applied in 1981 by Hideo Komada in Japanese Nagoya Research Institute, as he laid the groundwork for rapid prototyping systems using photopolymer [1].

Rapid prototyping allowed doctors to manufacture "surgical planning prototypes" for preoperative simulation, as well as for proper fitting and positioning, then the Rapid Manufacturing concept has emerged with more applicable capabilities, by allowing the production of fully customized and functional parts that can be used in the implantation surgery [1].

The distinction between Rapid Prototyping and rapid manufacturing is a pivoting point to ensuring the proper understanding of the importance of each concept role in the hip implant procedure [1].

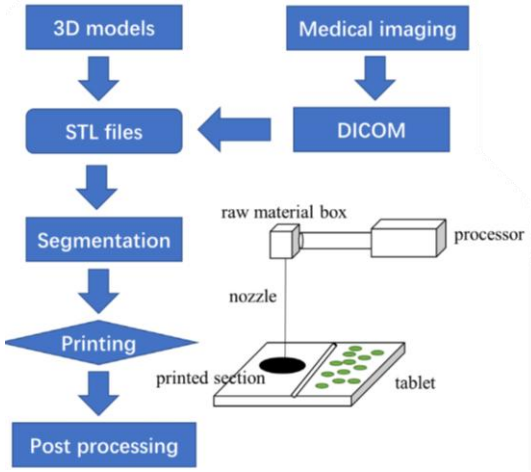

Figure 1.8. Simplified medical field additive manufacturing process flowchart [1].

As the steps and the needs of both rapid prototyping and rapid manufacturing may differ, there comes also the difference between users explained in the following points:

1- The Rapid Prototyping concept application in the medical feild comes from mastering the fitting regardless of the final finish, which is in breif attribiuted to the geometrical correctness of the final printed part, and as illustrated in the figure below, the material selection can be arbitrary, but with the considerations of the common 3D printing problems like (Warping, distortion, delamination, etc.) [2][3].

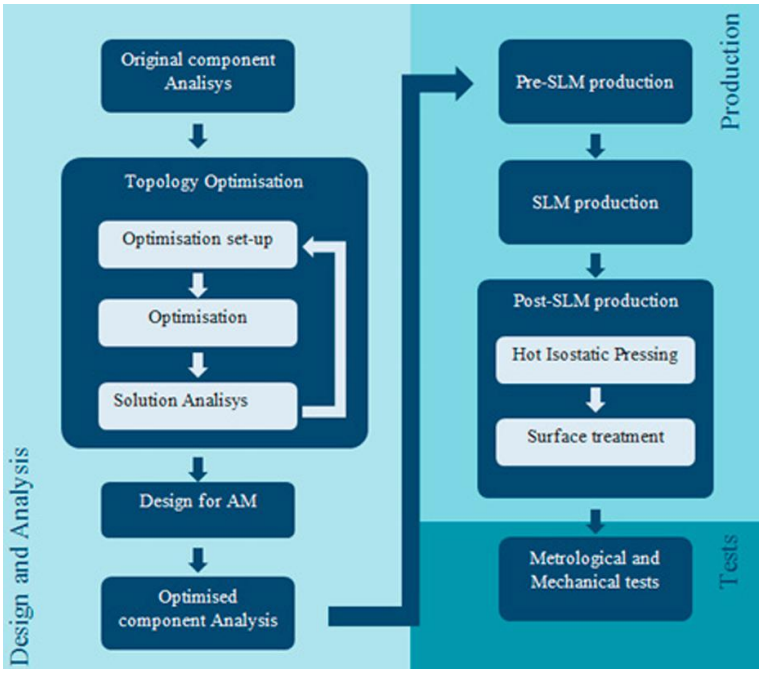

Figure 1.9. A Scheme of a 3D printing Procedure for Rapid Manufacturing [4].

2- In the Rapid Manufacturing concept application in the medical field the material selection is important, as it should be bio compatible material while also satisfieing , as well as considering the final fitting and the finishing, while also considering the common [2]. But since the technology that is implemented in this technique is different, Titanium alloy (Ti-6Al-4V) will be used in the, Topology Optimization of chapter 2, finite element analysis of this thesis in chapters 3 and 4.

However, when it comes to validation, since there has been no established automated quality control methods, that can be directly implemented in the usage of the 3D printed parts in both Rapid Prototyping or Rapid Manufacturing, a simplified flowchart below contains the steps for validation, from the transformation of the 3D model to an STL format file, until the final finish and the post processing of the part is completed [2].

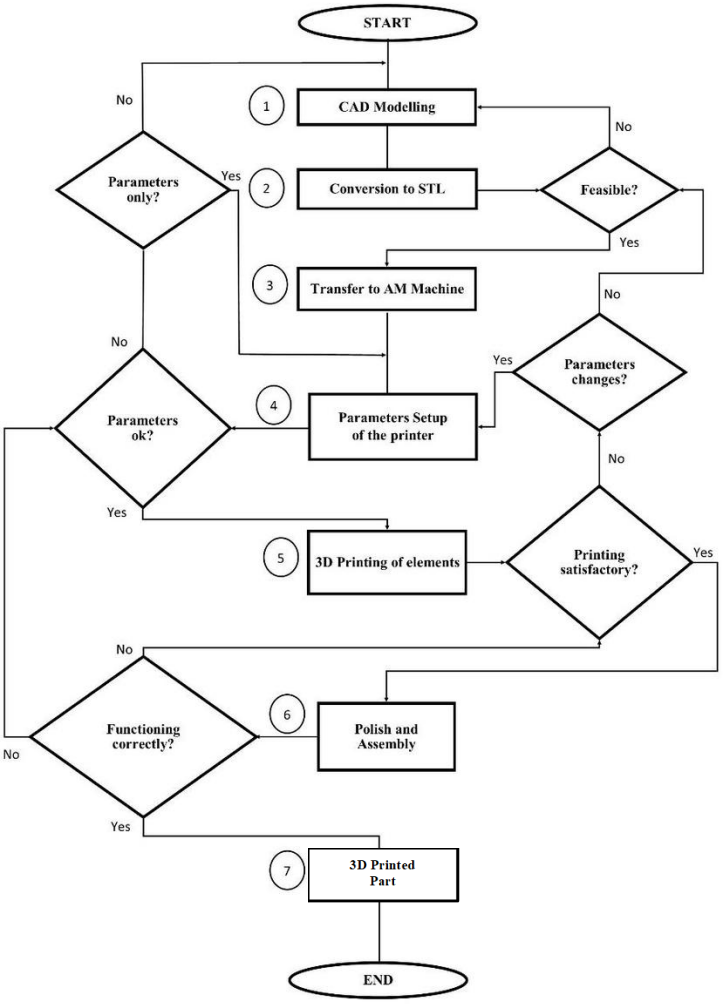

Figure 1.10. Validation Scheme of a 3D printing procedure for rapid prototyping mechanism [2].

While the development of Additive manufacturing technology has enabled the experimentation in medical application from the physical perspective, it is also important to realize the computational advances through the implementation of Topology Optimization, which goes further beyond the traditional CAD [2][4].

1.6 Topology Optimization and Generative Design

While traditional CAD requires the engineers to adhere to designing and drawing the geometry based on standard formulas and intuition, or experimentation that are extensive and expensive for both the time and the cost, the potential of Generative Design in additive manufacturing is critical to understand that it is driven by a computational methodology that is called the topology optimization, with the distinctive difference between the generative design and the topology optimization; is that generative design relies heavily on iterative approach of the application for the topology optimization, which means that even if the structure is mechanically optimized but it still has to be also the best of a lot of iterations, depending on the quality of the study, which studies multiple profiles that can also withstand the same mechanical loads and boundary conditions that are set to simulate the environment of testing in a digital environment [6].

The option of Generative Design is already available in many CAD/CAE software environments; but it is important to understand that Topology optimization computational method of which it is possible to obtain the results of a generative design [5].

Based on the applied boundary conditions, and the requirements of the preserved interfaces of the part, the topology optimization works to reduce the material in the segments where it is not efficient in the structure, by using a numerical analytical method to detect zones that have no displacement, which is embedded in the generate function in the Solid Edge [5]. In other words, the mathematical framework allows for a better distribution of the material in the necessary sections of the part [6].

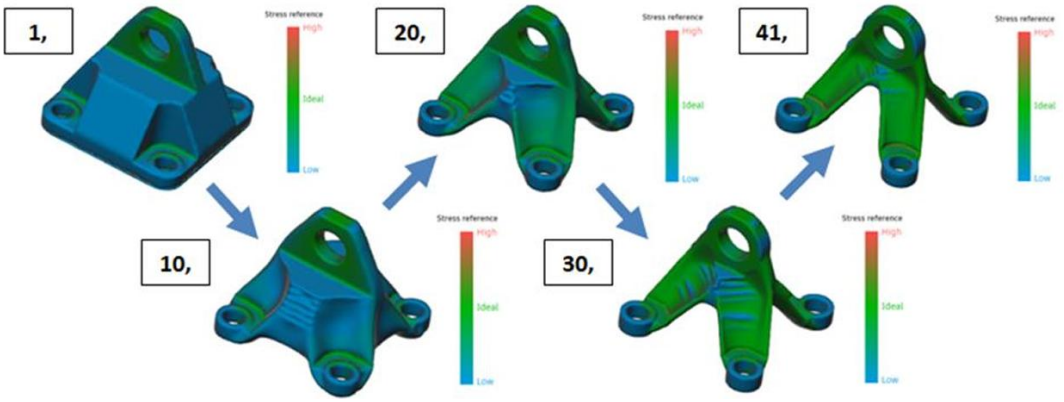

Figure 1.11. Generative Design Iteration Process [6].

It is also important to realize that topology optimization in other environments of simulation does not only allocate the material in the needed zones but can also have the possibility of creating additional structures, that are outside the original volume, which sometimes results in adding more mass of the material than the original form of the part [6].

By directly relying on the results of the FEA simulation and the boundary conditions, which includes the loads and the fixation with the supporting surfaces

in the form of sliding along the surface, as well as any other mechanical loads (like pressure or gravity etc.), that the part is subjected to, with the important step of the selection of the material, and the possibility of defining different properties than the ones that are available in the simulation environment, which can help to simulate more realistic results for deformation in case of the material that are in the form of alloys, or in case of stainless steel, after defining the carbon composites [6].

It is also possible to design the manufacturing technique as an evaluation method for the process of constructing and producing the part using generative design module that is applied in Fusion 360 CAM software, as the simulation is able to produce report with the nonconformities and deficiencies in the structures before testing it for production physically [6].

1.7 Physiological Loading Standards

In the recent advances in the field of patient specific hip implant design, it has been studied conducted by Alkentar and Mankovits [24][25]. Standardized physiological loads from Bergmann research have been implemented on par with machine learning in order to reduce the extensive computational resources of FEA iterative loops, Data set has mapped the input parameters for the density of the lattice structures, the cell size, and the weight of the patient, to output the von mises stress and displacement results for the mechanical behavior studying [22][23].

In order to achieve the most accurate simulation for the mechanical behavior inside the finite element analysis environment for the hip implant, the environment must be controlled and precisely conditioned in order to replicate the in vivo human activities using the boundary conditions. The ortho load database has been the source for the Bergmann standard as we also load database is considered to be globally recognized and studied a lot of physiological hip contact forces in order to represent various activities such as walking climbing and stumbling [23]. The setup for the generative design has to be designed with a high safety factor in order to allow the final geometry for the generative designed prosthesis to withstand the loads that the part is subjected to during the FEA testing.

Figure 1.12. Hip Implant III Used for Telemetry DAQ [28].

And the importance for applying these standardized multiaxial forces comes to evaluating the stress distribution across the stem of the hip implant as well as to estimate the fatigue life or the longevity of the part [22].

The age, weight, and height will be taken into consideration when doing the static and dynamic FEA simulation from Bergman standards for the loads of hip implant, and not the full list the subjects will be included due to the wide range of activities that will be tested during the dynamic analysis which includes: Walking, going up and down on the stairs, as well as in the case of stance, which means shifting the weight from two legs to one leg [27].

1.8 Simulation Setup and Data Acquisition

Accuracy and clinical relevance of the testing parameters in the simulation environment for the finite element analysis is important to produce computationally and biomechanically reliable results, with the main emphasis on the amount of data that can be applied as boundary conditions [27].

Figure 1.13. In Vivo Joint Dataset Collection [28].

Bergmann standards have implemented more than just the basic requirements of mechanical testing environment but also has wedged the gap between the biomechanical requirement for testing and the physical data acquisition sensors [27]. By developing the testing standards for the in vivo joint friction moment and contact forces, as well as developing the complex and advanced hip implants that have the possibility of being equipped with internal telemetry sensors in order to collect data about the physical activities in real time, which has led to the formation of the database on OrthoLoad, that eventually became the standardized physiological loads gold standard globally recognized dataset [27].

Before the implementation of computational simulations, researchers and engineers have used mathematical equations and models, or static loads to resemble the body weight while using multiplications for the simulation of safety factor, in order to simulate the acting forces on hip joints [27]. However, due to the highly complex dynamic activities of human that distribute the forces on multi axial vectors, it is important to carry on with the dynamic load simulation as the potential of static simulation does not fulfil the same category [27].

1.8.1 Static Simulation Telemetry Dataset:

Activity: Standing, lifting weight.

Parameter:

Lifting 20, 40, and 60kg.

Patients: H9L.

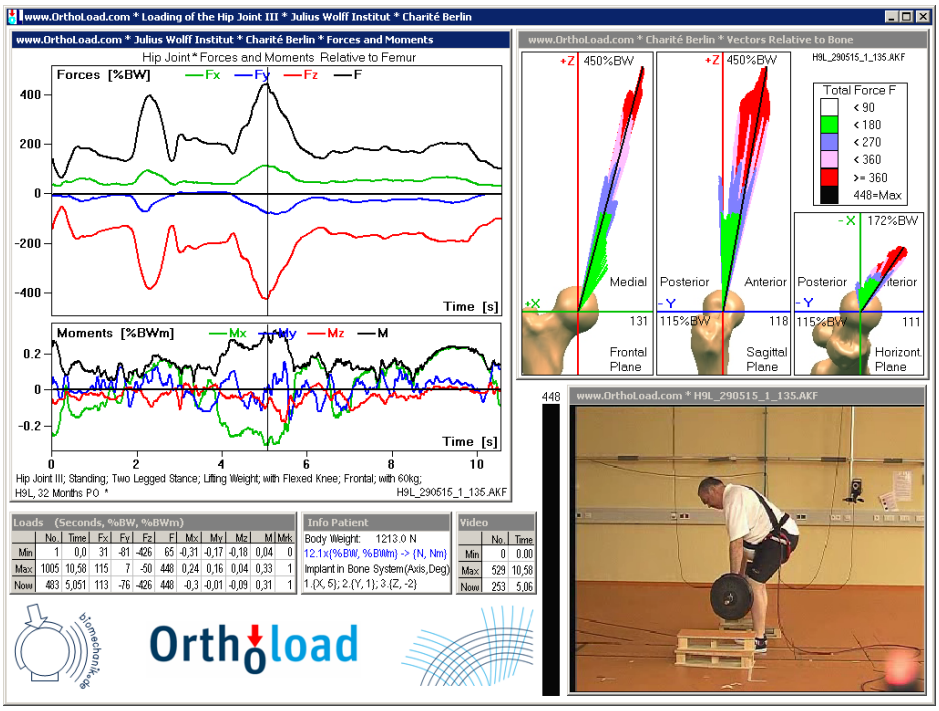

Figure 1.14. Hip Implant In Vivo Telemetry Peak Force and Setup (Static: Standing, Lifting 60Kg) [22].

1.8.2 Dynamic Simulation Telemetry Dataset:

Based on the available scenarios in OrthoLoads Database, here are the available parameters for dynamic activities when selecting the Activity:

Activity:

1- Walking (Level Walking).
2- Ascending Stairs (Stairs Up: Single Step).
3- Descending Stairs (Stairs Down: Single Step).

Patients: H4L. 2- H7R. 3- H9L

H: Hip

4,7,9: Subject Number

L/R: Left / Right

One of the very important characteristics of the OrthoLoad dataset is that it provides extremely wide details of wide range of human activities in connection

with the time-series data [27]. By implementing the data from the Bergmann standards, it is possible for researchers to apply forces in their axial components directly into the FEA simulation [27].

Figure 1.15. Hip Implant In Vivo Telemetry Peak Moment and Setup (Dynamic: Level Walking) [22].

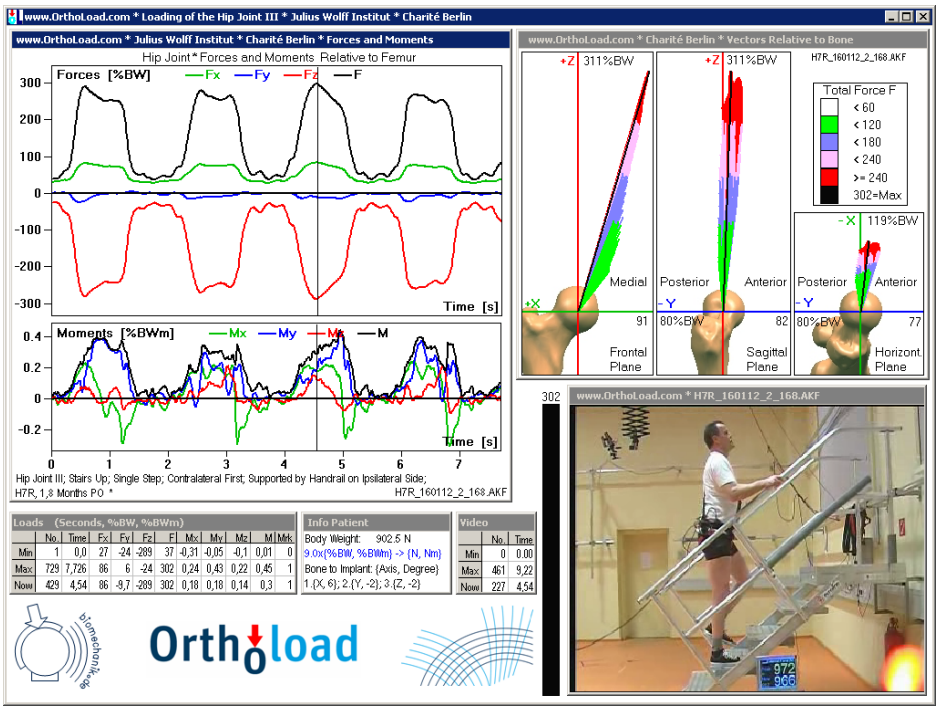

Figure 1.12. Hip Implant In Vivo Telemetry Peak Moment and Setup (Dynamic: Ascending Stairs) [22].

2 Design of Experiment (DOE) Generative Design and CAD Modelling

The experimentation of the generative design begins with the design of the hip implant in the 3D CAD environment. The selected software is Solid Edges student edition 2024. In the following steps, the validation scheme from the figure 1.10. will be adhered to in every step, as well as the steps of the work in the same order.

Starting with the selection of the parameter from an arbitrary model, as the focus of this thesis is not on the geometrical correctness of the model, or the proper customization of the part, but primarily on evaluation of integration of the manufacturing technique and the topology optimization methodology, as well as the characterization for the biomechanical responses.

So, for that: the simpler the design the less factors that can affect the ability to produce scientifically accurate results. The methodology is to select a simple geometry in order to develop the methodology, it is important to reduce the complexity of the geometry and limit the variables in order to produce scientifically accurate and reproducible results in the simulation environment, before proceeding with the complex anatomical model that resemble the realistic hip stem that can be found in the subchapter of 2.4.

2.1 Design of Experiment (DOE)

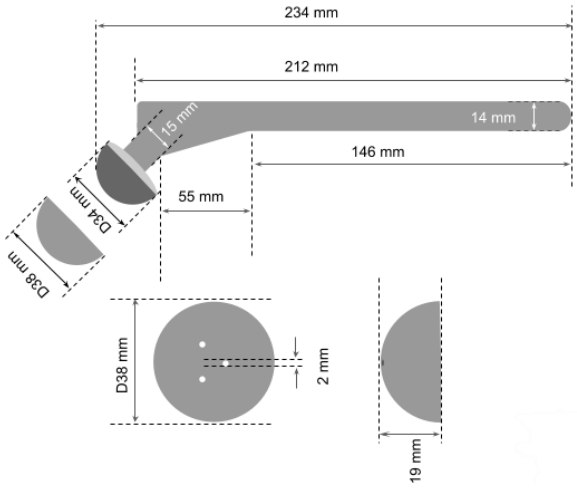

Figure 2.1. Selected hip implant Dimensions [16].

The geometry of the hip implant for the simplified femoral stem was designed using discrete dimensions with the overall height being 212mm, the neck angle with the shaft is 130°. The dimension of the femoral head being 38mm diameter, the selection of the femoral head diameter being important in order to control the centre of the mass for the assembly in the spatial geometry. These numbers can be considered to be the standard dimension for modular implants that are implemented in the cementless fixation practice for adult males.

As the femoral head being a preserved region, and since it's a module of design, it's out of generative design study target, the selection of the material will not be important; but it will still be considered for any computational factors or just to produce scientifically valid results.

Table 2.1 Boundary conditions application to the body

Category	Direction/ DOF	Amount	Placement
Force	Inferior	1600 N	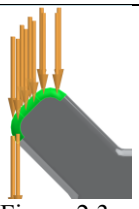 Figure 2.3. Force
Fixation	Zero Degrees of freedom	-	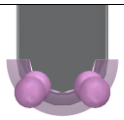 Figure 2.4. Base Fixation
Preserved regions	The femoral head connection region and the lower base	-	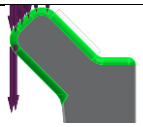 Figure 2.5. Femoral head preservation.  Figure 2.6. Base preservation.

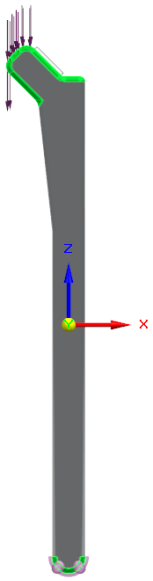

Figure 2.2. Boundary conditions placement

The following model is selected for the stem design of the hip implant, but the femoral head dimensions was modelled to control the exact dimensions of the geometry, then it is to be excluded from the generative design and the FEA in later steps. The boundary conditions are selected based on static loads and fixations and

the results of the generative design will be considered for the static FEA and the Dynamic FEA regardless of this factor. The material selection can be ceramics or Co-Cr-Mo alloys for the femoral head.

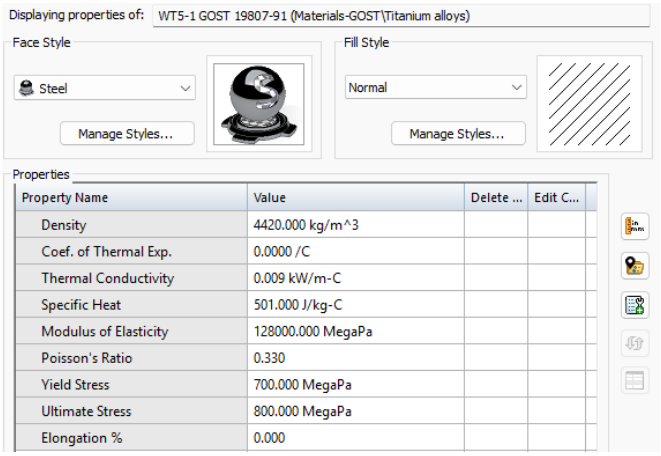

Figure 2.7. Material selection of the Generative study.

As the dynamic analysis methodology will consist of several static analysis possibilities, due to the fact that time series analysis does not measure the deformation in the whole body, it does instead measure the susceptibility of fatigue by creating a surface analysis on which segments of the model is bearing the amount of load similar to a histogram but imprinted on a 3D model.

The boundary conditions selection has been determined based on physiological boundary conditions that resemble extreme conditions of static loads and fixation scenarios, which in turn is important to initiate the generative design study based on semi realistic conditions. Setting the constraints and the boundary conditions at this stage of experimentation as well as defining the forces with their direction, are both important in order to allow the software algorithms to dictate the allocation of the material and map the stress both ways to decide the safe removal of the material from some part of the structure without sacrificing this structural integrity in the digital CAD model.

The applied load discussed in the table below is to simulate the forces on the hip joint during static scenario with an average weight of patient is approximately 80Kg, when splitting the weight on two legs, it results in approximately 40Kg, Considering the safety factor of 2, the static load is Inferior (Negative Superior) direction of 1600N value on the Z axis, In order to simulate the weight of the body pressing on to the pelvis. This scenario is during a static two legged stance and the 1600N is accounted to compensate for the dynamic spikes during the movement.

Static analysis will contain the load scenario for different standing positions we have variable weight in order to simulate the variable loads, and the dynamic analysis will be discussed in chapter 4, with the force direction and magnitude

altering between continuous cycles of load, and different load scenarios based on physical activity and sport activity.

The applied force is important in addition to the fixation in cementless application as the end of the stem is pressed against the bone with tight fit, so in order to replicate the result for that, Fixed constraint with 0° of freedom was applied to the lower base of the stem. With the final goal of preventing any translation (movement along the x,y, or z Axes), in order to allow the titanium stem to absorb the entire amount of load and to be distributed along the neck or the body.

2.1.1 CAD Modelling and Material Properties

After the establishment of the boundary conditions the parameters of the stem geometry and the material selection has been defined, the selection for the material was limited to the available library of the solid edge, choosing the closest equivalent to the medical standard of Ti-6Al-4V in WT5-1 GOST 19807-91 titanium alloy.

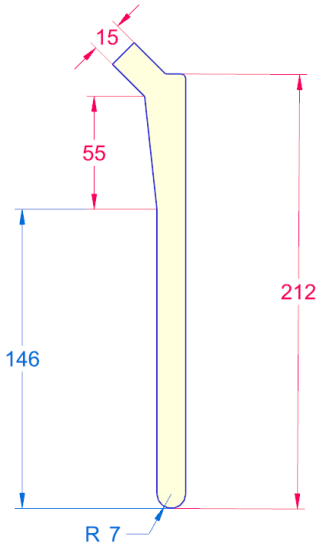

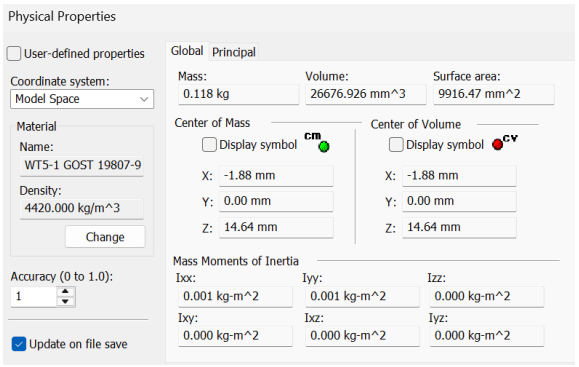

Figure 2.8. & Figure 2.9. Parameters of the 3D Design.

The thickness of the body has been selected as 8mm according to the parameter selection in Figure 2.1. with rounding features of 2 mm around the perimeter of the front and the back faces of body, then in the rest of the edges the round is 5 mm to avoid sharp angles and to compensate for the tolerance of 0.01 mm at the manufacturing phase.

Short 90° angle corners have been reduced completely in this structure, as they are considered to be areas of stress concentration where most of the cracks occur in cyclic fatigue loading conditions. When eliminating these geometrical features, the stress on the 90° angles corners is dissipated over continuous surface area.

2.1.2 Computational Setup

It is important to refer to the capabilities of the used computer as it heavily influenced the results of the generative study. Running the generative design topology optimization, FEA pre- & post- /processing, and CAD modelling of the hip implant geometry, was set up on this preconfigured machine, that was specifically made for design and rendering, which gives a solid framework and reliable results for the carried study.

Table 2.2. Computational Machine Steup

Item	Specification
Laptop model	Lenovo Yoga 14IRH8
CPU	Intel Core i5-13500H Raptor lake 7nm
Total Cores	12 (8 Efficient-cores at 3.5 GHz max)(4 Performance-cores)
RAM	16 GB DDR5 (13.7 GB Usable) 5200 MT/s
GPU	NVIDIA GeForce RTX 3050 (Mobile) 6GB VRAM
Storage	SSD NV Me M.2
Display & System	14-inch 3K | Windows 11 (64-bit)

As for the generative design study, the initial results were successful, with lower quality, so in the first documented study, it is a s follows:

2.1.2.1 Generative Study 1.1

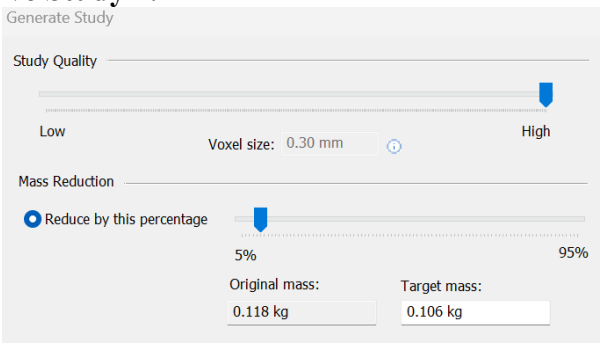

Figure 2.10. Parameters of the Generative Design Study 1.1.

The selection of the highest quality for the study at 300, which has an automatic control for the parameter of the voxel size 0.30 that has a pre-requisite additional offset that has been selected as 1.50 [mm].

The study did not conclude, but after running for more than 23 minutes, the software has frozen and stopped responding, due to the lack of RAM capacity, as the available size.

2.1.2.2 Generative Study 1.2

The study parameters has adjusted accordingly to compensate for the imitation of the current machine, with a lower quality study at 100 and a 0.43 mm voxel size, as well as a target weight reduction of 10% (From 0.118kg to 0.106kg), it ran for only 2 minutes before outputting the following results:

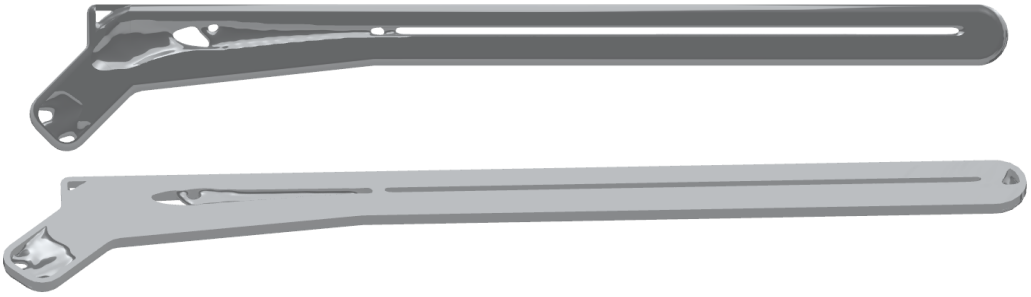

Figure 2.11.& Figure 2.12. Generative Study 1.2 Results with a sliced section.

It is important to realize that the development of the inner channels in the stem, which does not only appear on the surface of the stem, but it also develops in the inner channels, which is only visible when we create the sliced section.

However, due to the limitations that are with the current machine the results could be improved by using the ANSYS software topology optimization, the requirement for the machine will increase, but this will be utilized in the further sections of this thesis. But for now, from these results, it is possible to assume that the creation of inner channel is beneficial for the installation of hip implant in a cementless fixation as the inner channels allow for the ongrowth and ingrowth of bone tissues, which can be considered as an achievement towards the implementation of additive manufacturing in the hip implant procedure that are generatively designed.

For the following chapters, the simulation of finite element analysis will take place on a different model after it has been further enhanced for the implantation procedure with the design, keeping in mind that the final goal is not just to reduce the weight, but also to create channels inside the stem which are beneficial to give lighter weight and interesting features as discussed before.

2.1.2.3 Generative Study 1.3

Result that included further weight reduction has allowed 30% weight reduction with bigger channels, and more interesting results in the inner channels, which can be visibly seen without having to slice the model.

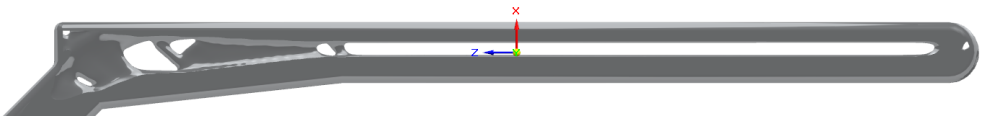

Figure 2.13. Generative Design Study 1.3 Results.

2.2 CAD Model Redesign

The initial design for the CAD model for the development of the methodology for the simulation set-up was done in order to ensure that the methodology of the work it's applicable and the results can be obtained when running the simulation, Then the second phase for the simulation which replicates the hip implant features that are very close to the real implant. As illustrated in the figure below; this design features real example for the implant stem which is the selection for both the static and the dynamic simulation FEA simulation.

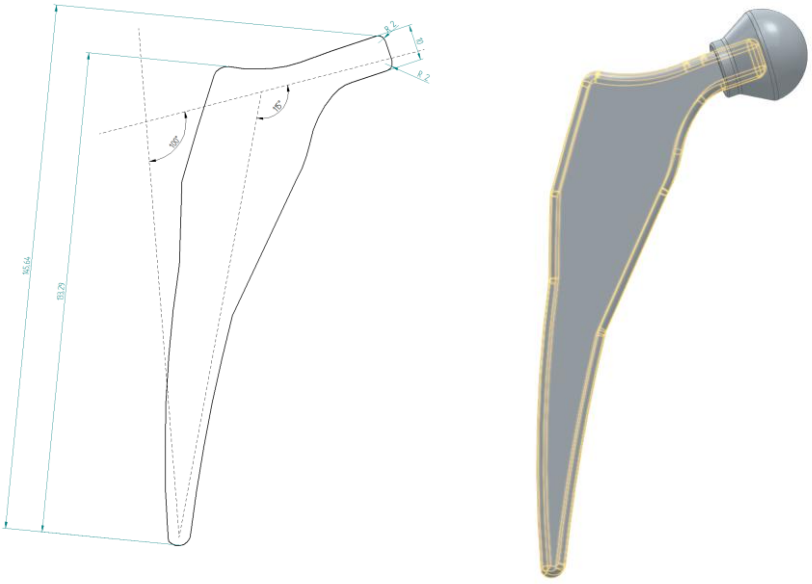

Figure 2.14. Redesigned CAD Model.

For that the model from the studies of the design features were designed according to the studies that were in the research of Dr Mankovits and Dr Alkentar. The simulation initial set-up was carried on in the environment of Solid Edge from the design of 3D model for the system as well as the features for the femoral head. With the plan for the boundary conditions to be selected and defined in the topology optimization study inside the environment of ANSYS.

However, for this chapter work it is only important to make the generative design model as well as the following step, to implement inside the environment of ANSYS Discovery which is the topology optimization, and in order to produce reliable results that can carry on to the dynamic analysis, it is important to use rigorous load conditions and boundary conditions. So, the next logical step in the course of the simulation setup is to define the initial parameters for the FEA, simulation.

2.3 Generative Design Study 2

The femoral head and the femoral stem relationship has been selected to be bonded with the load condition to be similar to the one selected in this standards of testing as mentioned in the literature review, is it low direction is downwards on the Z axis, coming from the disk on the top, with distributed force over the disk surface to be 2300N, that requires a minimum safety factor of 2.0 and for that on the femoral head the direct contact has been selected.

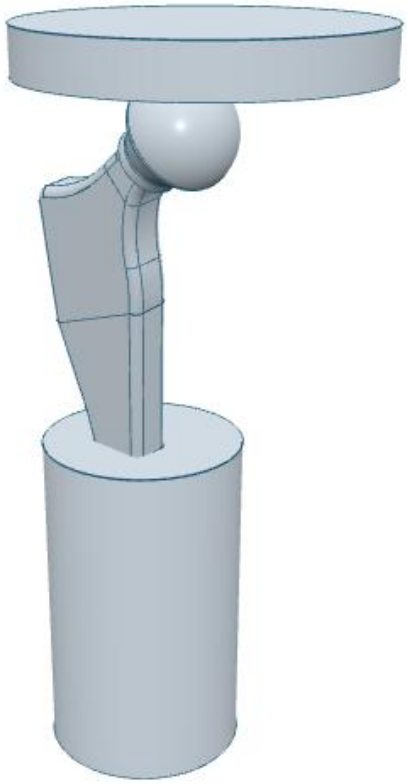

Figure 2.15. Simulation Setup for the CAD Model.

The faces of the femoral stem has been deliberately split it in order to provide better segmentation for the possibility of optimization in case of the generative design, as well as for the splitting of the surfaces due to the fact that the inner surfaces of the resin stand, which the femoral stem is fixed inside, are in direct contact with the surface of the latter, which requires the material of the resin to be fixed in case of the cylindrical shaped structure,

When designing the simulation setup to give the characteristics of the inner structure of the cylindrical shaped resin structure, the subtract function has been used so that the contact is exactly similar as if it was molded around the stem, which is the case of the Bergmann standard finite element analysis, that does also have the incline angle of 10° and the bending angle of 9°.

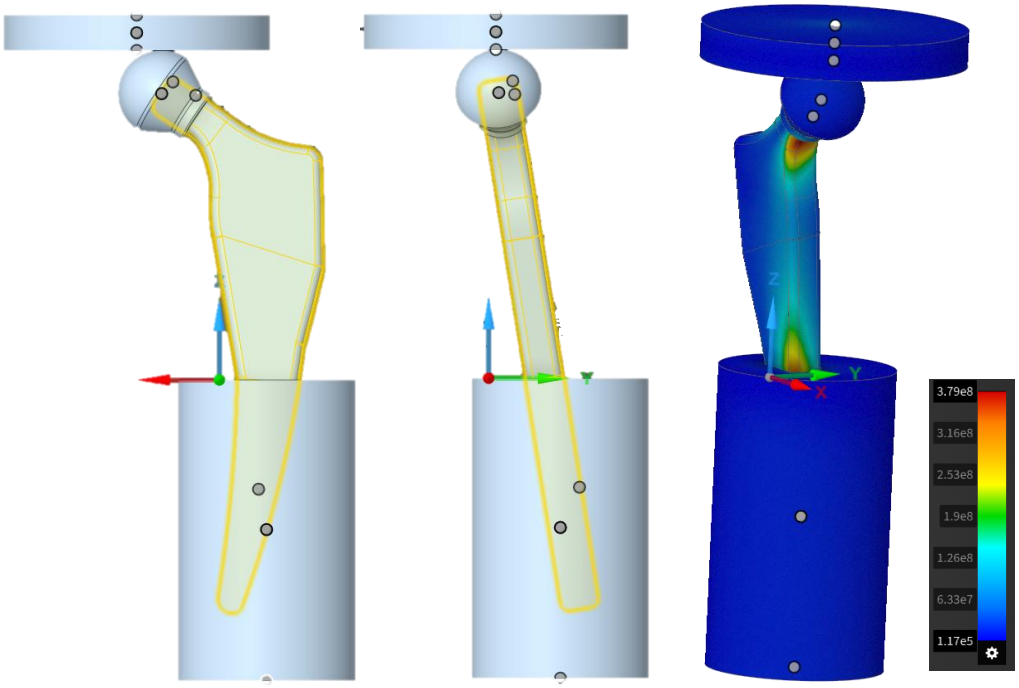

Figures 2.16., 2.17., 2.18. & 2.19. FEA (Bergmann Standard) Setup & FEA Results (Pa)

Topology optimization was done in the environment of Ansys discovery, which utilizes a new technology for meshless optimization in structural optimization loop. The final selection on the 25% weight reduction as the results that have been produced are far more reliable and superior to the ones of 30% weight reduction.

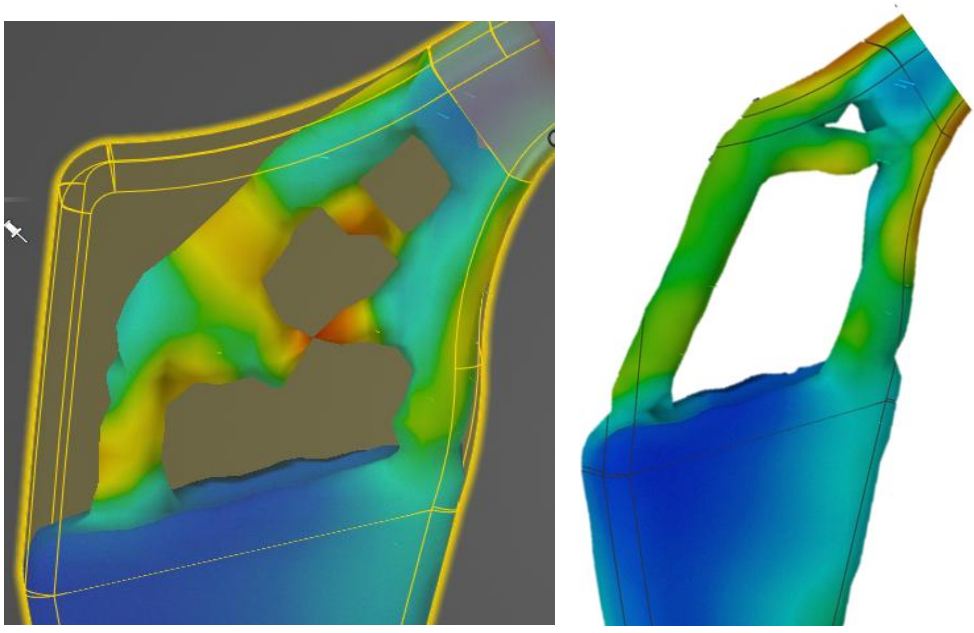

Figures 2.20., 2.21. 30 % Weight Reduction VS 25 % Weight Reduction.

2.4 Generative Design Study 3

It is important to note that the results from the ANSYS software are reliable, but it requires a lot of processing time and produces inconsistent results, so that, it is the ultimate choice to select the SolidEdge, as the Generative Design feature, is far more established, even if it lacks the advantages of the advanced computational capabilities, but for the results of this thesis, it is superior and reliable to proceed, with the current result, as it's already consistent for manufacturing, with superior channels., study quality has been set to the max, at 0.30mm voxel size, with the choice of mass reduction to be 25% (0.122 Kg to 0.092Kg).

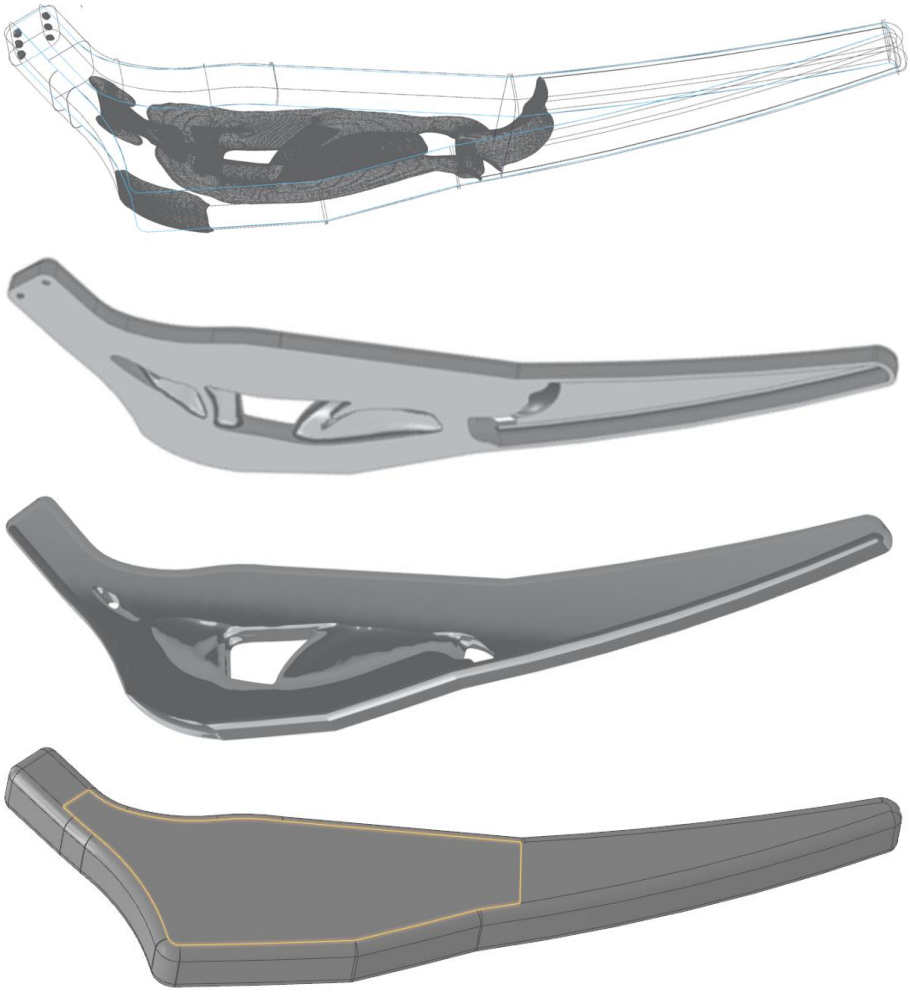

Figures 2.22., 2.23., 2.24., 2.25. & 2.26. Internal Channels (wireframe, sliced) in 25 % Weight in the selected face of the Original Hip Implant Model

The selection of the face for the generative design optimization that's taking place in the middle part of the hip implant stem, due to the fact that the initial stress testing has exerted signs for low stress distribution over this area, by face splitting, and taking the lines of the connection points from the fixation and the femoral head fixation point as the reference, to determine the optimal region for the split lines.

3 Static Finite Element Analysis Simulation

In the aftermath of the first Generative Design Study, And based on the future direction for both the thesis and the possibilities for extended work in the future, a new approach was realized for the model, based on the initial Generative design study and the possibility for the optimization, the reduction of 25% weight is the optimal condition for the finite element method simulation.

Following the standards from Bergmann developed work, which was discussed in the Literature review, the implantation is subjected to the variable static load for one patient profile, with the load and direction, or distribution along the vector force components being changeable, but the testing parameters and condition remaining the same for only one position of the stem.

The geometry has been fully designed to include the stem of the hip implant and the femoral head to increase the reliability of the final results. With the study being exclusively important to optimize and simulate the load on the stem.

3.1 Patient Anthropometric Profile Selection

Boundary conditions and specific patient profile information must be established been defined before starting the FEA simulation, in order to provide precise physiological simulation. The selection of the geometry is also important when performing the simulation which is why the second geometry that resembles the realistic femoral stem anatomically has been designed and selected.

Patient Profile (H9L)

In order to provide clinical viability to the highest possible degree, loads must be calculated accordingly. Patient profile and loads are directly sourced from the specific database of the globally recognized database of OrthoLoad, with the specific name of data set being in vivo telemetry data.

This specific data set was collected from a patient, with the code name: H9L, which resembles one of the most consistent light, to moderate, and then to extreme loading scenarios physically, in order to provide the optimized testing scenario to produce structurally sound results that can withstand extensive load cases.

The visible telemetry data for the selected patient has been selected from the Joint Load database of the OrthoLoad registry, by choosing the parameters as in the figure below:

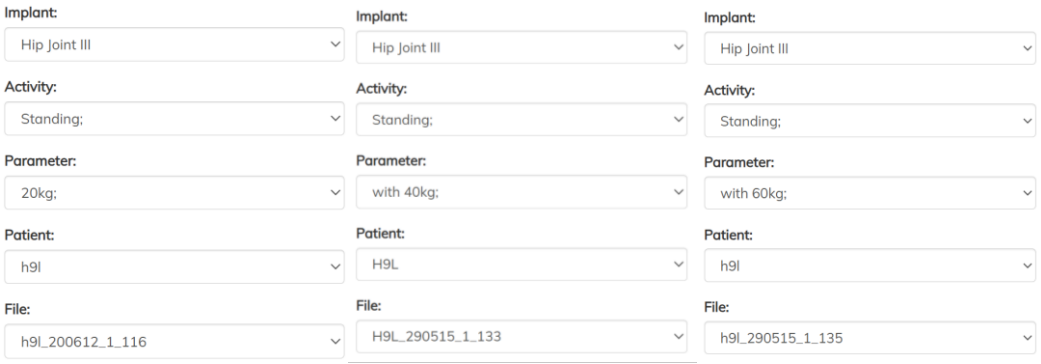

Figure 3.1. Joint Load Variables Selection [27].

The clinical Information and anthropometric profile of the patient is characterized as follows:

- Gender: Male.
- Age: 56 years old (54 years old at the time of THA).

Patient Physical Data:

- Height: 181 cm (1.81 m).
- Body Weight: 123.6 kg (Recorded as 1213 N during the specific test session).
- Telemetry DAQ Post-Op: 32 Months.

Other Medical Data:

- Body Mass Index (BMI): 37.7 kg/m² (Class II Severe Obesity)
- Medical Condition: Severe Coxarthrosis (Osteoarthritis of the hip joint).

The hip implant in the information from the anthropometric profile of the patient is a Hip Joint III, implanted in the left hip, with the time of telemetry data acquisition, after 32 months of the operation, which ensures that the implant has settled in order to withstand biomechanical loading naturally.

After the definition of the patient profile, the next logical step will be to introduce the approach for the simulation of Finite Element Analysis, in order to give a proper structure for the work of this thesis and organize the scenarios of distinctive testing as an experiment matrix, In 12 distinctive situations set-up, the simulation process will be split into static and dynamic, with the change of the dynamic having three different positions, and the static one having only single position with static load.

3.2 Static Simulation Matrix Determination

In order to give a comprehensive evaluation for the biomechanical performance and the structural integrity for the generative design stem and the baseline stem, the

process of designing the experiment is important in the beginning in order to avoid unreliable results goes by arbitrary numbers for the loads and the boundary conditions, the simulation methodology of highly controlled scenarios or divided into discrete bricks that will be in the structure of the FEA Simulations Workbench.

Testing scenarios have been derived directly from the telemetry database of OrthoLoads, with the categorization of the activity in case of walking, ascending the stairs, descending the stairs, as dynamic, standing, or lifting while standing as static.

For Patient H9L:

$W_{Total} = 1213\text{N}$ (Total Body Weight from Patient Weight: 123.6 Kg)

$W_{Torso} = 0.65 * 1213\text{N} = 788\text{N}$ (Patient upper body weight: 65% of W_{Total})

D_{Mucsle}= 0.05m (Perpendicular Distance from the Hip to the Muscle)

D_{load}= 0.15m (Horizontal Distance from the Hip to the Centre of Mass)

3.2.1 Deriving for the Peak Force (Standing and Lifting)

Based on the body weight multiplier that has been accurately calculated in the database of ortho load, the load peak has been calculated accordingly, in order to ensure accurate body-weight ratio.

Firstly, by calculating the Static Equilibrium of Moment on the hip joint:

$$\sum M_{Hip} = 0 \tag{1}$$

M_{Hip}: Moment of the hip joint [Nm]

$$F_{Muscle} * D_{Mucsle} = F_{Load} * D_{Load} \tag{2}$$

F_{Muscle}: Required Muscle Force to Lift [N]

F_{Load}: for the Required Force to Lift [N]

$$F_{Muscle} * D_{Mucsle} = (W_{Torso} + W_{Load}) * D_{Load} \tag{3}$$

$$F_{Muscle} = \frac{(W_{Torso} + W_{Load}) * D_{Load}}{D_{Mucsle}} \tag{4}$$

$$W_{load} = M[\text{Kg}] * g\ (9.81)\ [\text{N/m}^2] \tag{5}$$

By establishing the Total Joint Reaction Force equilibrium:

$$\sum F_y = 0 \tag{6}$$

$$JRF = F_{Muscle} + W_{Torso} + W_{Load} \tag{7}$$

3.2.2 Calculations for Scenario 1: Mild Load (20Kg)

Step 1: Calculating the Load:

$$W_{load\ 20} = 20Kg * 9.81 = 196.2\ \text{N}$$

Step 2: Calculating the Required Muscle Force:

$$F_{Muscle\ 20} = \frac{(W_{Torso} + W_{Load\ 20}) * D_{Load}}{D_{Mucsle}}$$

$$F_{Muscle\ 20} = \frac{(788 + 196.2) * 0.15}{0.05}$$

$$F_{Muscle\ 20} = \frac{984.2*0.15}{0.05} = 2952.6\ \text{N}$$

Step 3: Calculating the Joint Reaction Force:

$$JRF_{20} = F_{Muscle\ 20} + W_{Body} + W_{Load\ 20}$$

$$JRF_{20} = 2952.6 + 788 + 196.2$$

$$JRF_{20} = 3936.8\ \text{N}$$

3.2.3 Calculations for Scenario 2: Moderate Load (40Kg)

Step 1: Calculating the Load:

$$W_{load\ 20} = 40Kg * 9.81 = 393.4\ \text{N}$$

Step 2: Calculating the Required Muscle Force:

$$F_{Muscle\ 40} = \frac{(W_{Torso} + W_{Load\ 40}) * D_{Load}}{D_{Mucsle}}$$

$$F_{Muscle\ 40} = \frac{(788 + 393.4) * 0.15}{0.05}$$

$$F_{Muscle\ 40} = \frac{1180.4*0.15}{0.05} = 3541.2\ \text{N}$$

Step 3: Calculating the Joint Reaction Force:

$$JRF_{40} = F_{Muscle\ 40} + W_{Torso} + W_{Load\ 40}$$

$$JRF_{40} = 3541.2 + 788 + 393.4$$

$$JRF_{40} = 4721.6\ \text{N}$$

3.2.4 Calculations for Scenario 3: Extreme Load (60Kg)

Step 1: Calculating the Load:

$$W_{load\ 60} = 60Kg * 9.81 = 588.6\ \text{N}$$

Step 2: Calculating the Required Muscle Force:

$$F_{Muscle\ 60} = \frac{(W_{Torso} + W_{Load\ 60}) * D_{Load}}{D_{Mucsle}}$$

$$F_{Muscle\ 60} = \frac{(788 + 588.6) * 0.15}{0.05}$$

$$F_{Muscle\ 60} = \frac{1376.6*0.15}{0.05} = 4130\ \text{N}$$

Step 3: Calculating the Joint Reaction Force:

$$JRF_{60} = F_{Muscle\ 60} + W_{Body} + W_{Load\ 60}$$

$$JRF_{60} = 4129.8 + 788 + 588.6$$

$$JRF_{60} = 5506.4\ \text{N}$$

3.2.5 Simulation Matrix Determination

The JRF number for the load peak is extremely high compared to load mass and human body weight, as reasonably both of them would be considered to be around 1200 in case of 60 kilograms lifting scenario, but the musculoskeletal system in the human body does not carry weight as if it was on a beam, the lever distance just stick it in place horizontally and perpendicularly to the hip joint in order to estimate the exact amount of load peak in the place between the femur and acetabulum.

Table 3.1. Parameters and Scenarios for Static Simulation

Properties / Scenario	Lifting load Mass (M_{load}) [Kg]	Load Weight (W_{Load}) [N]	Load Peak *(JRF)* [N]
Scenario 1 Mild	20 Kg	196.2 N	3800N
Scenario 2 Moderate	40 Kg	393.4 N	4600N
Scenario 3 Extreme	60 Kg	588.6 N	5500N

3.3 Simulation by Mesh Convergence

Due to the fact that that topology optimization conceded with the results of the simulation carrying 5500 N, and produced the results without needing to mesh the model, it is important that selection of the mesh is done before the simulation, which only relies on the voxel size, and the following selections will be for the experimentation in order to count the convergence rate and see the fluctuation in the results.

3.3.1 Course Mesh (5.0mm)

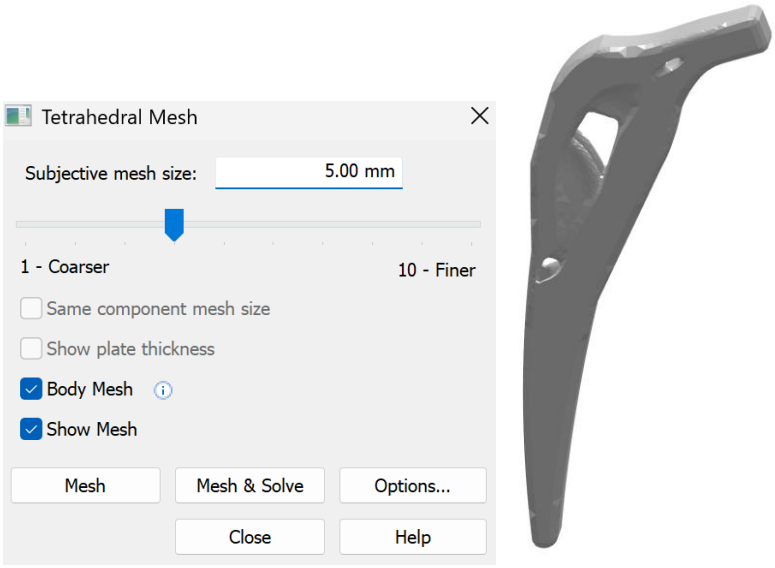

Figures 3.2. & Figure 3.3. Mesh Selection and Body Mesh.

3.3.1.1 Scenario 1. Course Mesh (5.0mm)

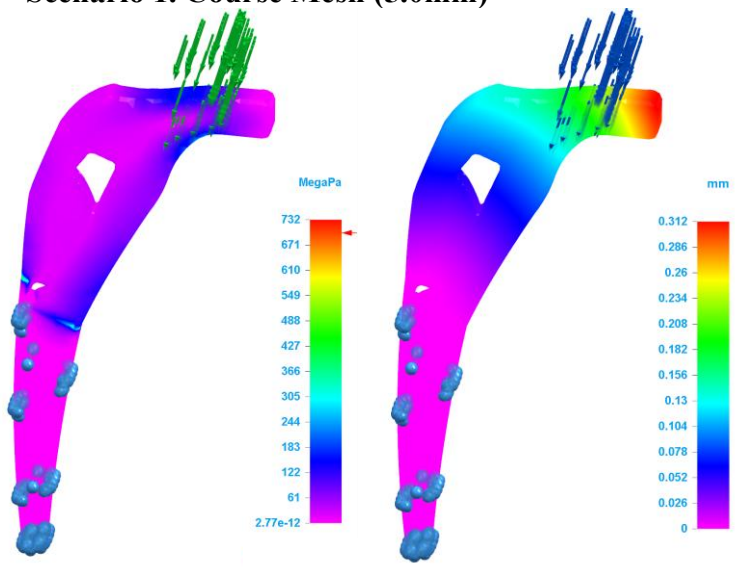

Figures 3.2. & Figure 3.2. Scenario 1 Stress and Displacement Simulation (Mesh 5mm)

3.3.1.2 Scenario 2. Course Mesh (5.0mm)

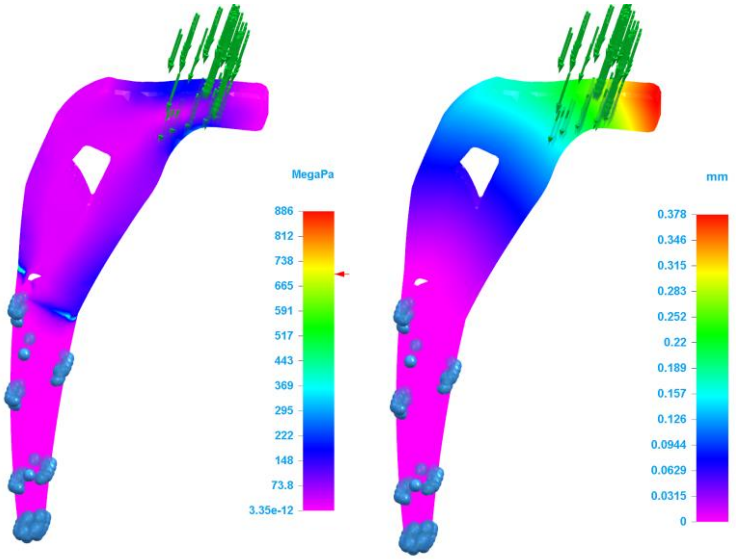

Figures 3.2. & Figure 3.2. Scenario 2 Stress and Displacement Simulation (Mesh 5mm)

3.3.1.3 Scenario 3. Course Mesh (5.0mm)

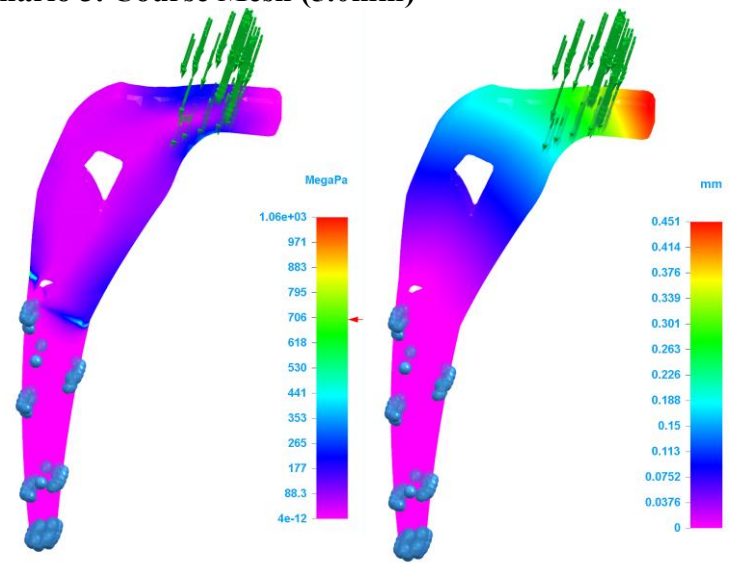

Figures 3.2. & Figure 3.2. Scenario 3 Stress and Displacement Simulation (Mesh 5mm)

The first experiment with 5mm mesh size has concluded with unreliable results that can produce safety factor for the 1st and 2nd scenarios, with a minimum 0.9, which is considered to be a failure, but the extreme scenario 3 as a resulted in only the production of the results of 1 as a safety factor due to the bottleneck of the mesh size, and for that the experiment is extended with the second mesh size of 2mm. In cases of 60Kg, 40Kg and 20Kg.

3.3.2 Moderate Mesh (2.0mm)

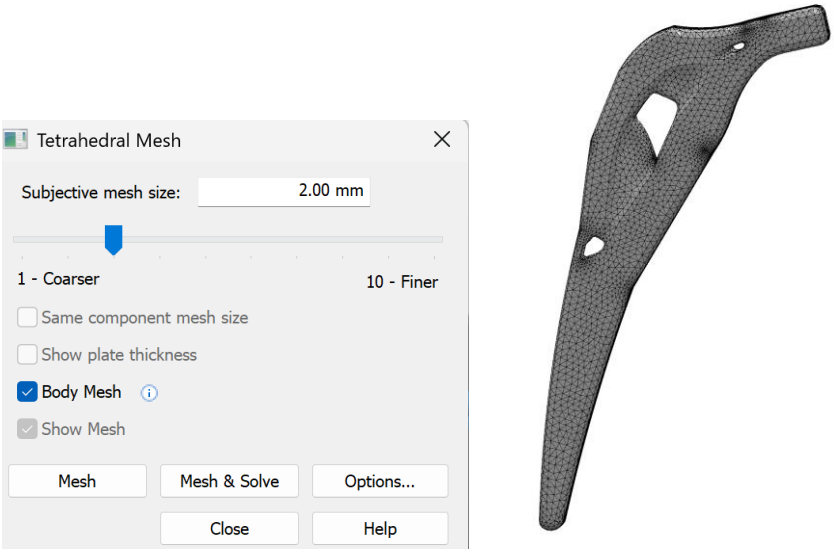

Figures 3.4. & Figure 3.5. Mesh Selection and Body Mesh.

3.3.2.1 Scenario 3. Moderate Mesh (2.0mm)

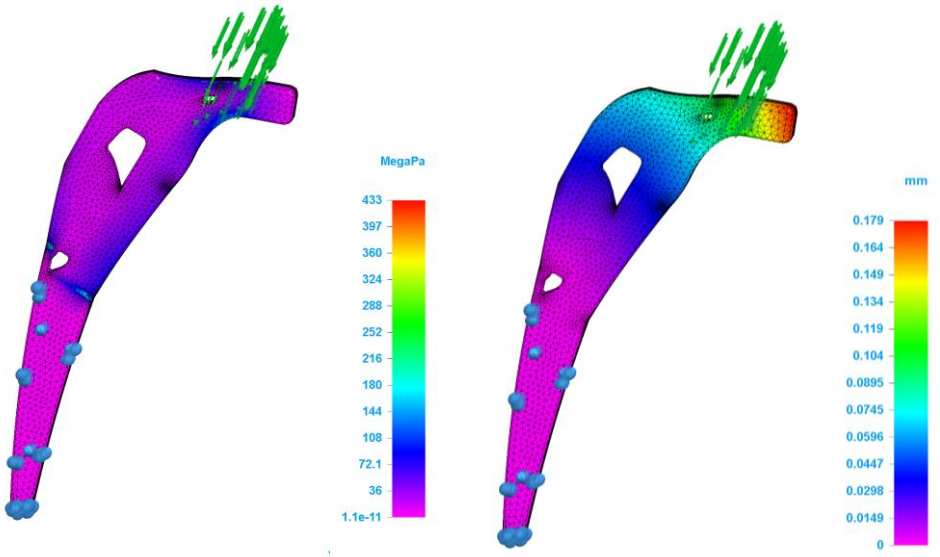

Figures 3.6. & Figure 3.7. Scenario 3 Stress and Displacement Simulation (Mesh 2mm)

Selection of the mesh for 2mm produced promising results that can be carried on for the dynamic finite element analysis, so the simulation carried on for scenario 2, and scenario 1, in order to ensure the consistency of the results before concluding findings. Safety factor results also have shown an improvement with the increase from 1.0 to 1.69 in the extreme scenario of 60kg weightlifting.

3.3.2.2 Scenario 2. Moderate Mesh (2.0mm)

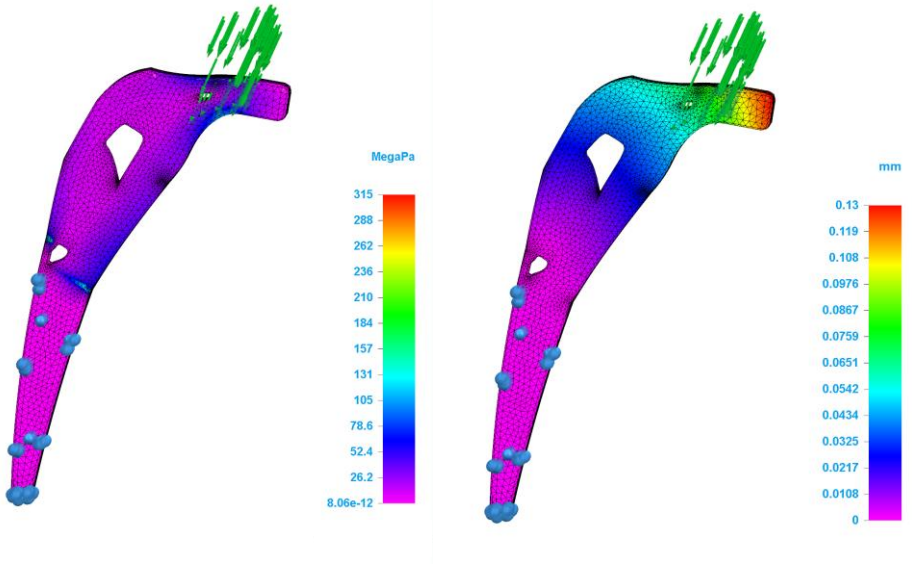

Figures 3.8. & Figure 3.9. Scenario 2 Stress and Displacement Simulation (Mesh 2mm)

3.3.2.3 Scenario 1. Moderate Mesh (2.0mm)

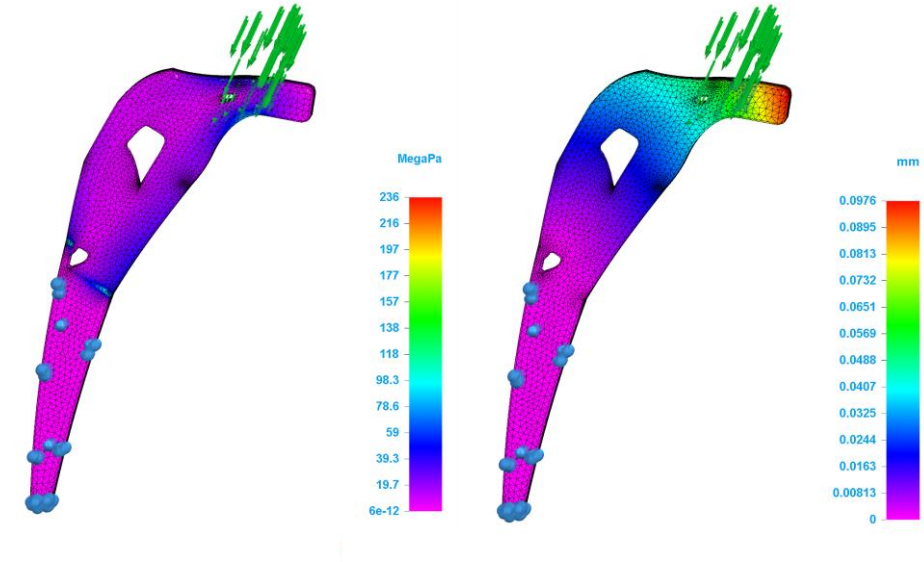

Figures 3.10. & Figure 3.11. Scenario 1 Stress and Displacement Simulation (Mesh 2mm).

An improvement has also been seen in the results of the first and second scenario with the yielding stress going below the required one for a minimum safety factor of 2.0 as 360 MPa to 315 MPa, in scenario 2, and 236 MPa, in scenario 1.

Following the successful establishment of the methodology from the Generative Design optimization to the static finite element simulation, it is safe to say that 2mm mesh size is the selection for further simulations in case of the dynamic simulation using the same generative designed model.

4 Dynamic Finite Element Analysis Simulation

It was successfully demonstrated that the generative designed hip implant can withstand an extreme amount of load, in the worst cases. However, in order to ensure that the implant can obtain clinical certification, it is important to study the cyclic events, where human locomotion is considered to be important as the active adult averages 1-2 million step cycles per year. So, it is important to study the cyclic loading, as even continuous loads that are below the material's yield strength, can cause the initiation of microscopic cracks, that can propagate overtime due to the repetition of the movement.

4.1 Patient Anthropometric Profile Selection

Multiple profiles have been selected for the experimentation with the subject H9L already established in the previous chapter, two more profiles have been added for the simulation of the three activities that have also been established in the final part of the literature review. The selection has been based on the mechanical forces diversity in order to capture the human locomotive activities that cover the majority of the repetitive cycles in the daily life of an active human.

The In Vivo telemetry data is the primary source for the cyclic loads that would be performed in the dynamic simulation. However, mathematical calculations will be carried on in order to ensure the proper ground rules for reliable testing results.

It is important to note that the acquisition of this data was not directly taken from the source, but it was derived through the telemetry data (.akf) measurement files from the specific selection of the implant type, as well as the activity with the measurement on the selected side of the hip, in case of the stairs ascending and descending, the activity selection was inverted in order to ensure that the same results are being received as illustrated below in in the figure 4.1 and 4.2, with the only distinction between the two patient profiles: is that one of them had the surgery of the hip implantation in the left hip, and the other in the right one.

The clinical Information and anthropometric profiles of the selected patients for the dynamic FEA simulation are characterized as follows:

Patient Profile (H9L) - Level Walking Activity

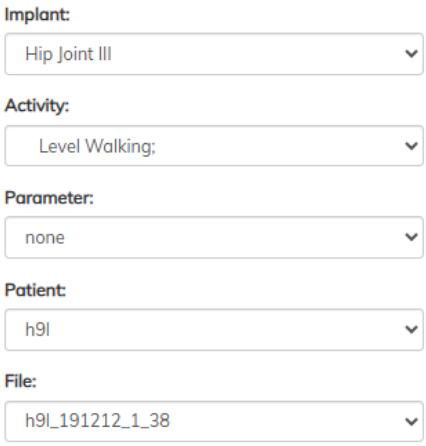

Figure 4.1. Dataset Selection for Joint Load Variables (H9L) [27].

- Gender: Male
- Age: 56 years old (54 years old at the time of THA)

Patient Physical Data:

- Height: 181 cm (1.81 m).
- Body Weight: 123.6 kg (Recorded as 1213 N during the specific test session).
- Telemetry DAQ Post-Op: 32 Months.

Other Medical Data:

- Body Mass Index (BMI): 37.7 kg/m² (Class II Severe Obesity)
- Medical Condition: Severe Coxarthrosis (Osteoarthritis of the hip joint).

Patient Profile (H7R) - Ascending Stairs Activity

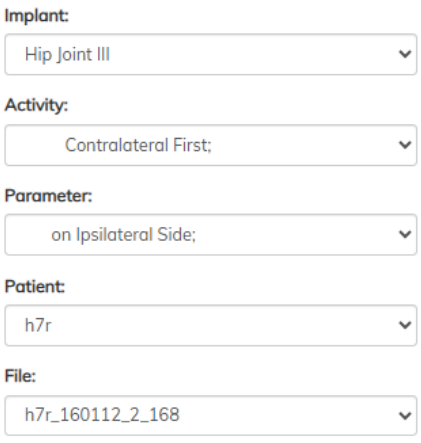

Figure 4.2. Dataset Selection for Joint Load Variables (H7R) [27].

- Gender: Male

- Age: 52 years old (50 years old at the time of THA)

Patient Physical Data:

- Height: 179 cm (1.79 m).
- Body Weight: 92.0 kg (Recorded as 902.5 N during the specific test session).
- Telemetry DAQ Post-Op: 18 Months.

Other Medical Data:

- Body Mass Index (BMI): 28.7 kg/m² (Overweight)
- Medical Condition: Severe Coxarthrosis (Osteoarthritis of the hip joint).

Patient Profile (H4L) - Descending Stairs Activity

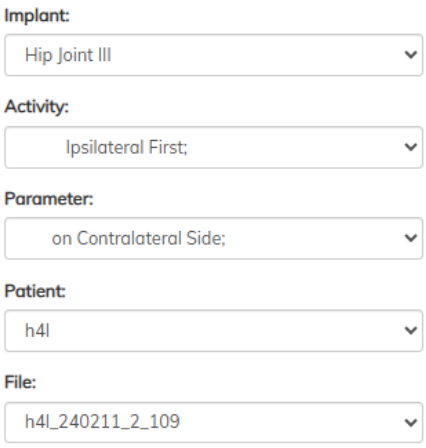

Figure 4.3. Dataset Selection for Joint Load Variables (H4L) [27].

- Gender: Male
- Age: 50 years old (49 years old at the time of THA)

Patient Physical Data:

- Height: 178 cm (1.78 m).
- Body Weight: 81.5 kg (Recorded as 799.5 N during the specific test session).
- Telemetry DAQ Post-Op: 10 Month.

Other Medical Data:

- Body Mass Index (BMI): 25.7 kg/m² (Slightly Overweight).
- Medical Condition: Severe Coxarthrosis (Osteoarthritis of the hip joint).

4.2 Dynamic Load Matrix Determination

As dynamic activity increases the complexity with adding momentum and acceleration it is not possible to implement a similar approach for using the static

equation $M = F \times D$, as when the vector component distribution and decomposition; two equations will be used in order to evaluate the components of the forces which are the dynamic equilibrium and the 3D vector distribution.

The static equilibrium that was established in chapter 3 using the moment equilibrium $\sum M = 0$ to calculate the boundary conditions for the lever system equilibrium. So, in order to calculate the mass acceleration for the multidirectional shifting of the center of gravity for the human body, and the momentum, the Joint Reaction Force will be calculated at the peak of each 3 (t) main points of each dynamic activity.

Starting with the initial state of the joint reaction force calculation that was established in chapter 3:

$$JRF_{Static} = F_{Muscle} + W_{Body} + W_{Load} \tag{8}$$

$$F = m_{Body} \times a_{Dynamic} \tag{9}$$

By incorporating the second law of motion for Newton of dynamic equilibrium, as well as by considering the patient's gravitational body weight and the muscular tension that is required to balance the forces on the joint. The forces inertia there is affected by acceleration can be calculated using:

The inertia force as a vector form can be expressed for the dynamic equilibrium as:

1. The inertia force component is derived:

$$\vec{F}_{Inertia}(t) = m \times \vec{a}(t) \tag{10}$$

2. From the total dynamic equilibrium:

$$\sum \vec{F}\,(t) = m \times \vec{a}(t) \tag{11}$$

3. In order to calculate the joint reaction force in the dynamic form:

$$J\vec{R}F_{Dynamic}(t) = \vec{F}_{Muscle}(t) + \overrightarrow{W}_{Body} + \vec{F}_{Inertia}(t) \tag{12}$$

However, the database has the results of the force components already present in the dataset for each activity cycle, including the information about the time, and the distribution of the load for the force components in the X, Y, and Z directions.

So, in order to express the dynamic force vector resultant in every point of activity over the selected scenarios, the following expression is used:

$$\vec{F}(t) = \begin{bmatrix} F_x(t) \\ F_y(t) \\ F_z(t) \end{bmatrix} \tag{13}$$

$\vec{F}(t)$: Force Vector at (t) [N]

$F_x(t)$: Force Lateral Component at (t) [N]

$F_y(t)$: Force Posterior/Anterior Component at (t) [N]

$F_z(t)$: Force Inferior/Superior Component at (t) [N]

The resultant force magnitude can be calculated in the following equation:

$$F_{Resultant}(t) = \sqrt{F_x(t)^2 + F_y(t)^2 + F_z(t)^2} \tag{14}$$

$F_{Resultant}(t)$: Force Resultant Component at (t) [N]

Calculating the body weight ratio for each scenario, using the following equation:

$$\lambda(t) = \frac{F_{Resultant}(t)}{\mathrm{W_{Body}}\ (P)} \tag{15}$$

λ: Body Weight Multiplier

P: Patient Body Weight

4.2.1 Patient Body Weight calculations

The weight has been obtained from the physical data available in the dataset for the selected activities.

$$W_{Body}(P) = m * g \tag{16}$$

m: Body Mass [Kg]

$g = 9.81$ [N/m^2]

For Patient H9L:

$$\mathrm{W_{Body}(H9L)} = 123.6 * 9.81 = 1213 \text{ N}$$

For Patient H7R:

$$\mathrm{W_{Body}(H7R)} = 92 * 9.81 = 902.52 \text{ N}$$

For Patient H4L:

$$\mathrm{W_{Body}(H4L)} = 81.5 * 9.81 = 799.5 \text{ N}$$

4.2.2 Matrix A H9L (Level Walking)

Calculating the Scenario A1, Level Walking first phase (Heel Strike)

Step 1. Selection of the first time point in the walking cycle is around 15% of the cycle time (0.839 s) where the data has been recorded as follows:

$$\vec{F}(0.839) = \begin{bmatrix} 724.21\,\text{N} \\ -232.42\,\text{N} \\ -2901.36\,\text{N} \end{bmatrix} \quad \left| \begin{array}{c} F_x(0.839) = 724.21\,\text{N} \\ F_y(0.839) = -232.42\,\text{N} \\ F_z(0.839) = -2901.36\,\text{N} \end{array} \right.$$

Step 2. Calculating the resultant Force:

$$F_{Resultant}(0.839) = \sqrt{(724.21)^2 + (-232.42)^2 + (-2901.36)^2}$$

$$F_{Resultant}(0.839) = 2999.40\,\text{N}$$

Step 3. The correspondence body weight multiplier is:

$$\lambda\,(0.839) = \frac{2999.40}{1213}$$

$$\lambda\,(0.839) = 2.47$$

Calculating the Scenario A2, Level Walking second phase (Mid-Stance)

Step 1. Selection of the second time point in the walking cycle is around 30% of the cycle time (1.690 s) where the data has been recorded as follows:

$$\vec{F}_{A2}(1.690) = \begin{bmatrix} 992.28\,\text{N} \\ -429.22\,\text{N} \\ -3505.44\,\text{N} \end{bmatrix} \quad \left| \begin{array}{c} F_x(1.690) = 992.28\,\text{N} \\ F_y(1.690) = -429.22\,\text{N} \\ F_z(1.690) = -3505.44\,\text{N} \end{array} \right.$$

Step 2. Calculating the resultant Force:

$$F_{Resultant}(1.690) = \sqrt{(992.28)^2 + (-429.22)^2 + (-3505.44)^2}$$

$$F_{Resultant}(1.690) = 3668.38\,\text{N}$$

Step 3. The correspondence body weight multiplier is:

$$\lambda\,(1.690) = \frac{3668.38}{1213}$$

$$\lambda\,(1.690) = 3.02$$

Calculating the Scenario A3, Level Walking third phase (Toe Propulsion)

Step 1. Selection of the third time point in the walking cycle is around 48% of the cycle time (2.698 s) where the data has been recorded as follows:

$$\vec{F}(2.698) = \begin{bmatrix} 952.62\,\text{N} \\ -506.06\,\text{N} \\ -3616.97\,\text{N} \end{bmatrix} \quad \left| \begin{array}{c} F_x\,(2.698) = 952.62\,\text{N} \\ F_y(2.698) = -506.06\,\text{N} \\ F_z(2.698) = -3616.97\,\text{N} \end{array} \right.$$

Step 2. Calculating the resultant Force:

$$F_{Resultant}(2.698) = \sqrt{(952.62)^2 + (-506.06)^2 + (-3616.97)^2}$$

$$F_{Resultant}(2.698) = 3774.39\,\text{N}$$

Step 3. The correspondence body weight multiplier is:

$$\lambda\,(2.698) = \frac{3774.39}{1213}$$

$$\lambda\,(2.698) = 3.11$$

4.2.3 Matrix B H7R (Ascending Stairs)

Calculating the Scenario B1, Ascending Stairs first phase (Step-Up)

Step 1. Selection of the first time point in the stair ascent cycle is around 15% of the cycle time (1.157s) where the data has been recorded as follows:

$$\vec{F}(1.157) = \begin{bmatrix} 651.75\,N \\ -0.18\,N \\ -2157.88\,N \end{bmatrix} \quad \left| \begin{array}{c} F_x(1.157) = 651.75\,\text{N} \\ F_y(1.157) = -0.18\,\text{N} \\ F_z(1.157) = -2157.88\,\text{N} \end{array} \right.$$

Step 2. Calculating the resultant Force:

$$F_{Resultant}(1.157) = \sqrt{(651.75)^2 + (-0.18)^2 + (-2157.88)^2}$$

$$F_{Resultant}(1.157) = 2254.16\,\text{N}$$

Step 3. The correspondence body weight multiplier is:

$$\lambda\,(1.157) = \frac{2254.16}{902.5}$$

$$\lambda\,(1.157) = 2.50$$

Calculating the Scenario B2, Ascending Stairs second phase (Mid-Stance)

Step 1. Selection of the second time point in the stair ascent cycle is around 30% of the cycle time (2.320 s) where the data has been recorded as follows:

$$\vec{F}(2.320) = \begin{bmatrix} 500.68\ \text{N} \\ -122.08\ \text{N} \\ -1197.39\ \text{N} \end{bmatrix} \quad \left| \begin{array}{c} F_x(2.320) = 500.68\ \text{N} \\ F_y(2.320) = -122.08\ \text{N} \\ F_z(2.320) = -1197.39\ \text{N} \end{array} \right.$$

Step 2. Calculating the resultant Force:

$$F_{Resultant}(2.320) = \sqrt{(500.68)^2 + (-122.08)^2 + (-1197.39)^2}$$

$$F_{Resultant}(2.320) = 1303.59\ \text{N}$$

Step 3. The correspondence body weight multiplier is:

$$\lambda\,(2.320) = \frac{1303.59}{902.5}$$

$$\lambda\,(2.320) = 1.44$$

Calculating the Scenario B3, Ascending Stairs third phase (Final propulsion)

Step 1. Selection of the third time point in the stair ascent cycle is around 48% of the cycle time (3.711 s) where the data has been recorded as follows:

$$\vec{F}(3.711) = \begin{bmatrix} 262.64\ \text{N} \\ -\ 0.90\ \text{N} \\ -\ 239.22\ \text{N} \end{bmatrix} \quad \left| \begin{array}{c} F_x(3.711) = 262.64\ \text{N} \\ F_y(3.711) = -0.90\ \text{N} \\ F_z(3.711) = -239.22\ \text{N} \end{array} \right.$$

Step 2. Calculating the resultant Force:

$$F_{Resultant}(3.711) = \sqrt{(262.64)^2 + (-0.90)^2 + (-239.22)^2}$$

$$F_{Resultant}(3.711) = 355.26\ \text{N}$$

Step 3. The correspondence body weight multiplier is:

$$\lambda\,(3.711) = \frac{355.26}{902.5}$$

$$\lambda\,(3.711) = 0.39$$

4.2.4 Matrix C H4L (Descending Stairs)

Calculating the Scenario C1, Descending Stairs first phase (Initial Descend)

Step 1. Selection of the first time point in the stair descent cycle is around 15% of the cycle time (1.202 s) where the data has been recorded as follows:

$$\vec{F}(1.202) = \begin{bmatrix} 363.65\,\text{N} \\ -131.65\,\text{N} \\ -1098.46\,\text{N} \end{bmatrix} \quad \left| \begin{array}{c} F_x(1.202) = 363.65\,\text{N} \\ F_y(1.202) = -131.65\,\text{N} \\ F_z(1.202) = -1098.46\,\text{N} \end{array} \right.$$

Step 2. Calculating the resultant Force:

$$F_{Resultant}(1.202) = \sqrt{(363.65)^2 + (-131.65)^2 + (-1098.46)^2}$$

$$F_{Resultant}(1.202) = 1164.56\,\text{N}$$

Step 3. The correspondence body weight multiplier is:

$$\lambda\,(1.202) = \frac{1164.56}{799.52}$$

$$\lambda\,(1.202) = 1.46$$

Calculating the Scenario C2, Descending Stairs second phase (Load transfer)

Step 1. Selection of the second time point in the stair descent cycle is around 30% of the cycle time (2.404 s) where the data has been recorded as follows:

$$\vec{F}(2.404) = \begin{bmatrix} 309.18\,\text{N} \\ -89.49\,\text{N} \\ -999.61\,\text{N} \end{bmatrix} \quad \left| \begin{array}{c} F_x(2.404) = 309.18\,\text{N} \\ F_y(2.404) = -89.49\,\text{N} \\ F_z(2.404) = -999.61\,\text{N} \end{array} \right.$$

Step 2. Calculating the resultant Force:

$$F_{Resultant}(2.404) = \sqrt{(309.18)^2 + (-89.49)^2 + (-999.61)^2}$$

$$F_{Resultant}(2.404) = 1050.16\,\text{N}$$

Step 3. The correspondence body weight multiplier is:

$$\lambda\,(2.404) = \frac{1050.16}{799.52}$$

$$\lambda\,(2.404) = 1.31$$

Calculating the Scenario C3, Descending Stairs third phase (Stabilizing)

Step 1. Selection of the third time point in the stair descent cycle is around 45% of the cycle time (3.194 s) where the data has been recorded as follows:

$$\vec{F}(3.194) = \begin{bmatrix} 275.67\ \text{N} \\ -58.66\ \text{N} \\ -678.26\ \text{N} \end{bmatrix} \quad \left| \begin{array}{l} F_x(3.194) = 275.67\ \text{N} \\ F_y(3.194) = -58.66\ \text{N} \\ F_z(3.194) = -678.26\ \text{N} \end{array} \right.$$

Step 2. Calculating the resultant Force:

$$F_{Resultant}(3.194) = \sqrt{(275.67)^2 + (-58.66)^2 + (-678.26)^2}$$

$$F_{Resultant}(3.194) = 734.49\ \text{N}$$

Step 3. The correspondence body weight multiplier is:

$$\lambda\,(3.194) = \frac{734.49}{799.52}$$

$$\lambda\,(3.194) = 0.92$$

4.2.5 Matrix Determination

The data from the previous calculations has been collected in the table below, with the following step, to conduct the simulation of the following Scenarios, with the load distribution being on three phases of each scenario, on the form of multiple static FEA simulation to analyse the movement, that substitutes for the time series.

Table 4.1. Matrix of Scenarios and force load components for Dynamic Simulation

Scenario	F_x [N]	F_y [N]	F_z [N]	$F_{Resultant}$ [N]
A1	724.21	-232.42	-2901.36	2999.40
A2	992.28	-429.22	-3505.44	3668.38
A3	952.62	-506.06	-3616.97	3774.39
B1	651.75	-0.18	-2157.88	2254.16
B2	500.68	-122.08	-1197.39	1303.59
B3	262.64	-0.90	-239.22	355.26
C1	363.65	-131.65	-1098.46	1164.56
C2	309.18	-89.49	-999.61	1050.16
C3	275.67	-58.66	-678.26	734.49

4.3 Dynamic Simulation

4.3.1 Matrix A Simulation

Table 4.2. Matrix A of Scenarios for (H9L) and force load components for Dynamic Simulation

Scenario	F_x [N]	F_y [N]	F_z [N]	$F_{Resultant}$ [N]
A1	724.21	-232.42	-2901.36	2999.40
A2	992.28	-429.22	-3505.44	3668.38
A3	952.62	-506.06	-3616.97	3774.39

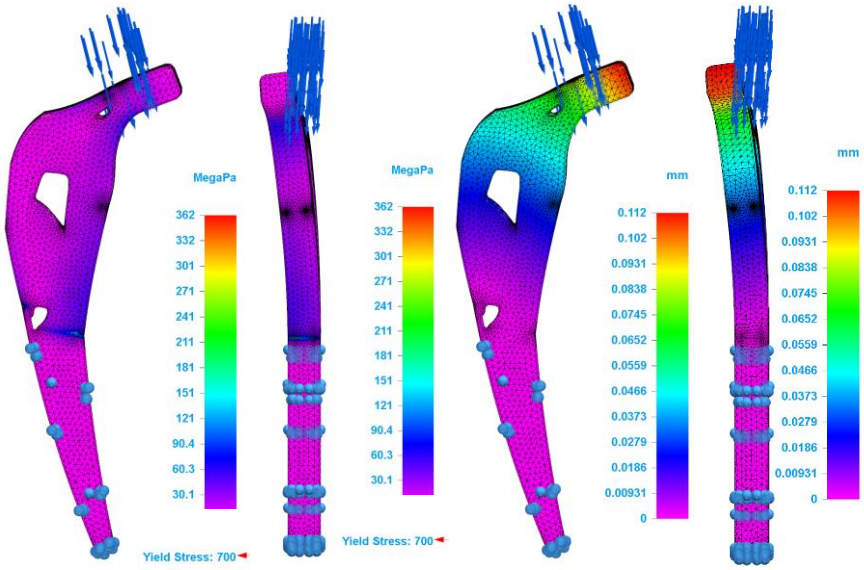

Figures 4.4., 4.5., 4.6. & 4.7. Scenario A1 Stress and Displacement (Front & Right Views).

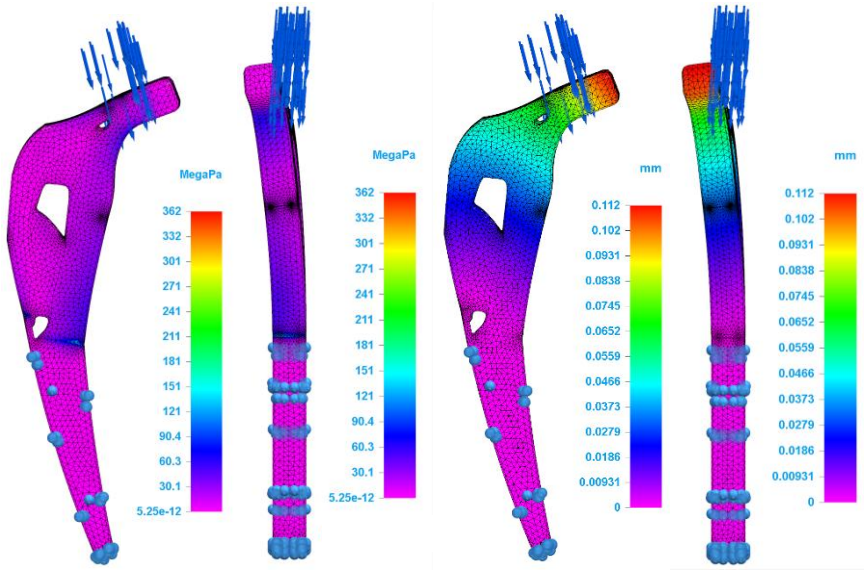

Figures 4.8., 4.9., 4.10. & 4.11. Scenario A2 Stress and Displacement (Front & Right Views).

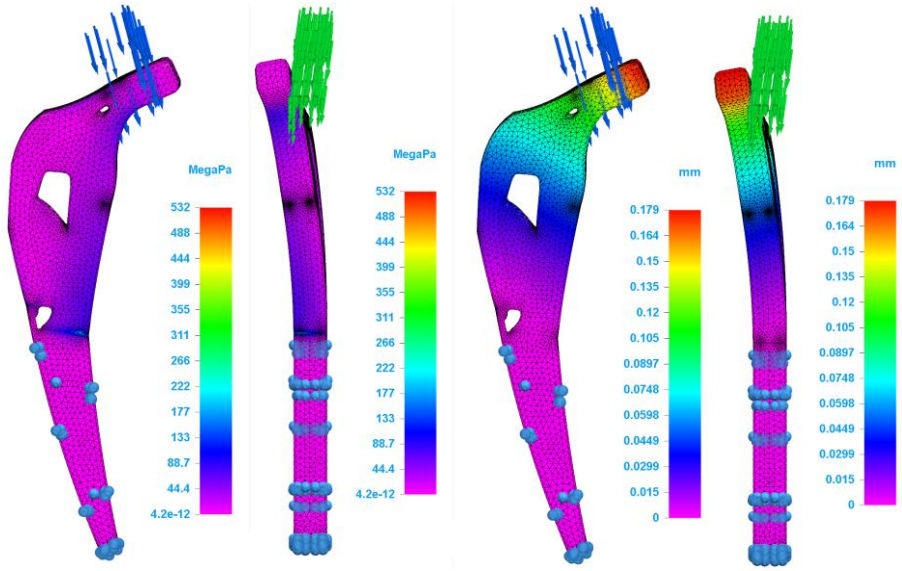

Figures 4.12., 4.13., 4.14. & 4.15. Scenario A3 Stress and Displacement (Front & Right Views).

4.3.2 Matrix B Simulation

Table 4.3. Matrix B of Scenarios for (H7R) and force load components for Dynamic Simulation

Scenario	F_x [N]	F_y [N]	F_z [N]	$F_{Resultant}$ [N]
B1	651.75	-0.18	-2157.88	2254.16
B2	500.68	-122.08	-1197.39	1303.59
B3	262.64	-0.90	-239.22	355.26

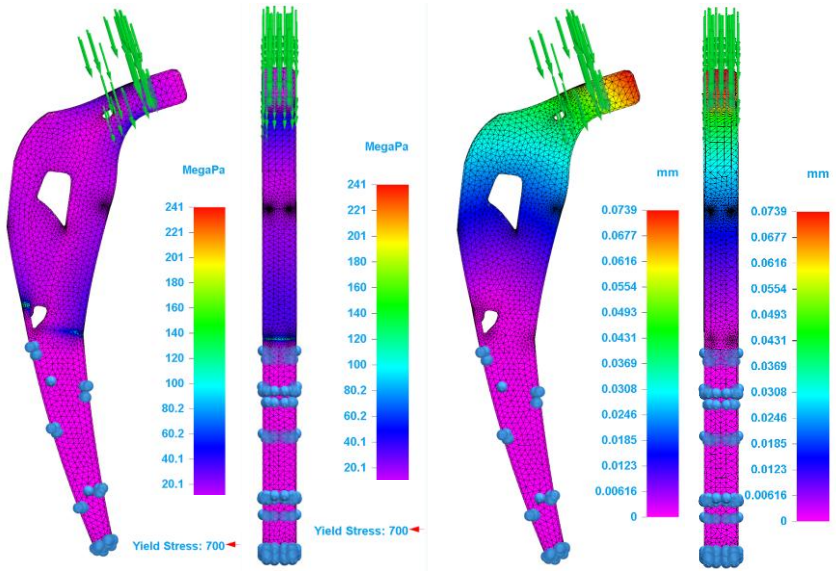

Figures 4.16., 4.17., 4.18. & 4.19. Scenario B1 Stress and Displacement (Front & Right Views).

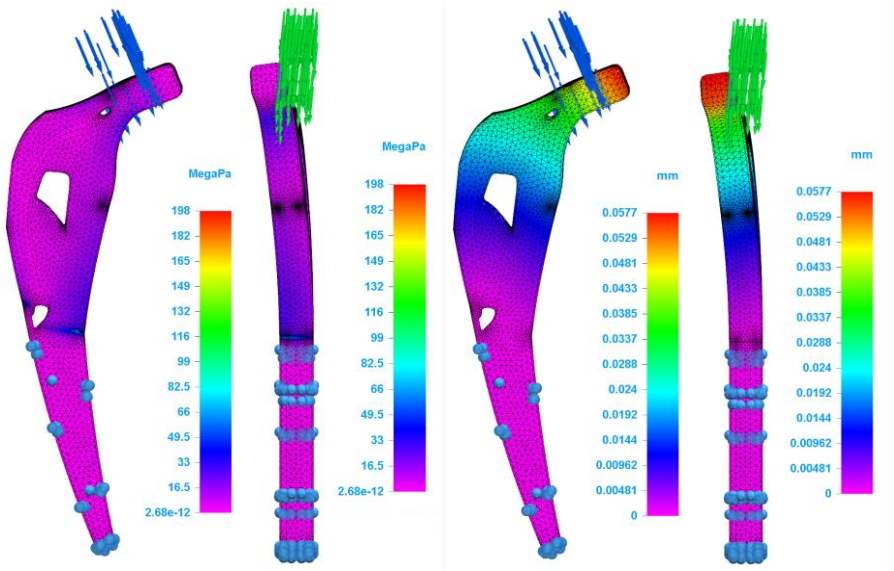

Figures 4.20., 4.21., 4.22. & 4.23. Scenario B2 Stress and Displacement (Front & Right Views).

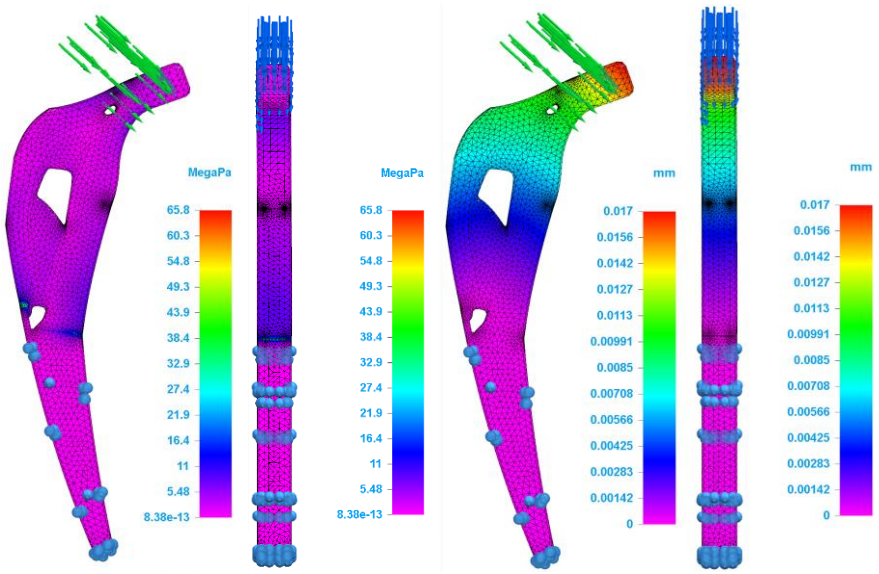

Figures 4.24., 4.25., 4.26. & 4.27. Scenario B3 Stress and Displacement (Front & Right Views).

4.3.3 Matrix C Simulation

Table 4.4. Matrix C of Scenarios for (H4L) and force load components for Dynamic Simulation

Scenario	F_x [N]	F_y [N]	F_z [N]	$F_{Resultant}$ [N]
C1	363.65	-131.65	-1098.46	1164.56
C2	309.18	-89.49	-999.61	1050.16
C3	275.67	-58.66	-678.26	734.49

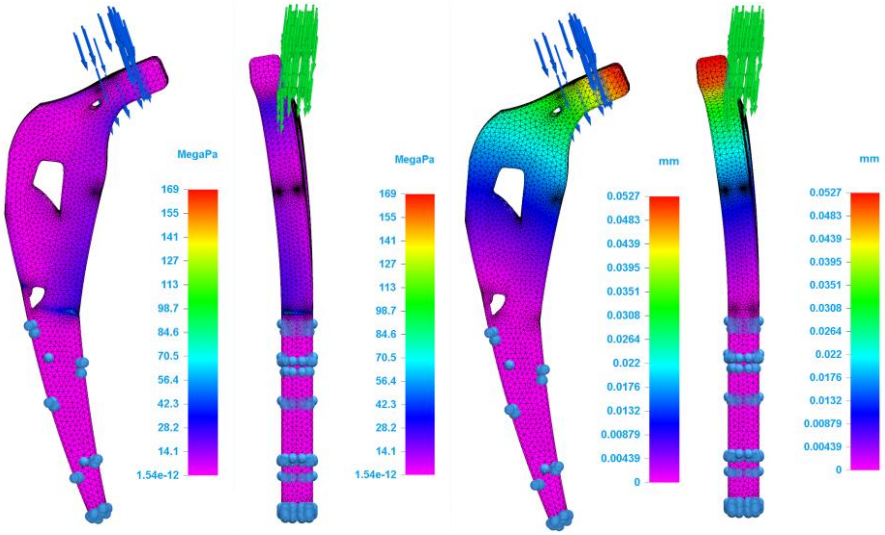

Figures 4.28., 4.29., 4.30. & 4.31. Scenario C1 Stress and Displacement (Front & Right Views).

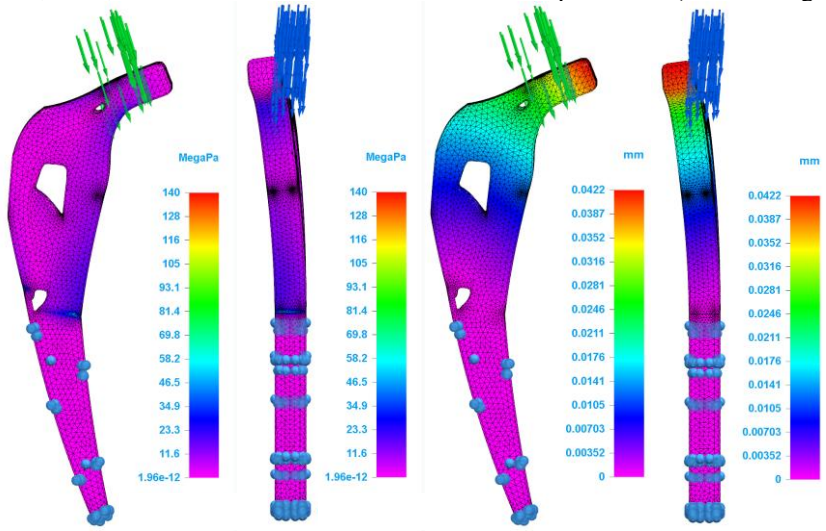

Figures 4.32., 4.33., 4.34. & 4.35. Scenario C2 Stress and Displacement (Front & Right Views).

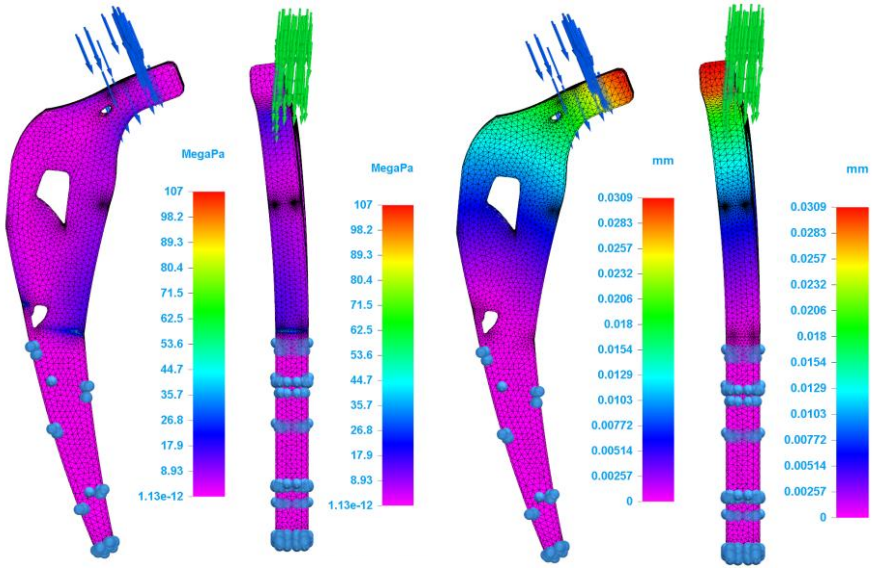

Figures 4.36., 4.37., 4.38. & 4.39. Scenario C3 Stress and Displacement (Front & Right Views).

5 Validation and Manufacturing Feasibility

This chapter discusses the findings of this thesis in order to transform the results into manufacturing assessments and manufacturability.

5.1 Validation Process

In order to realize the workflow and the computational optimization for the mass customized hip implants it is required to bridge the gap with the current manufacturing possibilities. The objective of this thesis was to design a hip implant system that can be optimized with generative design in order to achieve the weight reduction of 25%, with the consideration of safety factor and manufacturability. 2 validation framework tiers were followed, the initial validation was to computationally analyze the biomechanical behavior of the digital concept, and to apply and manufacturing assessment is the following step.

The testing parameters were derived from reliable telemetry data of in vivo OrthoLoad database for three patients profiles (H4L, H7R, H9L), in order to provide data that can be clinically relevant for biomechanical validation of the optimized hip implant stem, with the multi axial loads accurately replicated in cases of extreme static lifting, level walking and stair locomotion.

After the evaluation of biomechanical safety, the manufacturer ability of the generative stem is analyzed purely in a theoretical manner, in order to estimate the reliability of the production and the cost too. With the manufacturing hardware selection for manufacturing (5-axis CNC, and EOS M290 Direct Metal Laser Sintering (DMLS)). Using this integrated approach, it is possible to provide the conclusion that the generative design system can be feasible for manufacturing and possible to survive the hostile environment of the human body in order to provide the exact pathway to manufacture it.

5.1.1 Static Validation

In order to establish the structural integrity of the 25% weight reduction optimized generative designed prosthetic hip stem, The data that was derived from the telemetry data set and calculated in chapter 3, has been selected to be applied on the model in a static FEA study, that was divided on scenarios described in the matrix of the table 3.1. It is important to realize that static testing does not capture

the possibility for fatigue in human locomotion, but it's highly effective in order to identify the load bearing capacity in the geometry, as well as the stress concentration critical points in worst case scenarios.

Von Mises Stress Analysis For factor of Safety

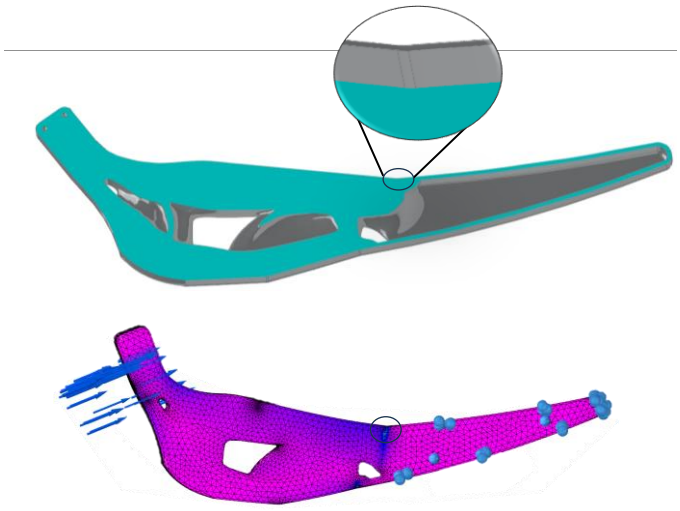

Figure 5.1 Stress concentration zone in a sliced view

Because of the internal features of the generative designed hip stem are completely round which helps to enable the distribution of the load equally on the surface, the results of the FEA static study has shown stress concentration over the medial neck junction chamfer, Which necessitates the need for full surface modeling in medical field application designs, in order to eliminate the stress concentration zones, by reducing every angle and visible connection lines in load bearing areas.

Under the maximum load bearing of 5500N, 433 MPa what's the maximum stress in this zone, which is compared to the 830 MPa yield stress of the titanium alloy Ti-6Al-4V (GOST 19807-91), gives the following safety factor based on the calculation:

$$FoS = \frac{\sigma_{yeild}}{\sigma_{max}} \tag{16}$$

Where:

FoS: Factor of safety

σ_{max}: The maximum Von Mises stress recorded [MPa]

σ_{yeild}: Tensile yield strength [MPa]

$$FoS = \frac{830}{433} = 1.9$$

Which means that even under the peak load of 5500N, the structure is able to withstand the extreme scenario 3, that was done in the static simulation. Keeping in mind that in engineering applications of the medical field, safety factor number between 1.5 and 2.0 is the requirement to account for the unpredictable variables, and the number of 1.9 safety factor exceeds comfortably the threshold for the absolute worst-case scenario.

For the reference of the moderate load of 40kg weightlifting scenario 2, the calculation for the safety factor is:

$$FoS = \frac{830}{315} = 2.6$$

5.1.2 Dynamic Validation

Von Mises Stress Analysis

Level Walking- Matrix A Simulation (For H9L)

The maximum von mises stress that was recorded in the toe propulsion phase of A3 scenario (t = 2.698s) simulation was 532MPa, resulting in a safety factor of 1.56, which means that the structure absorbed the impact in a severe case of obese patient, without localizing any yield, which means that the implants successfully absorbed the shift of the center of gravity. Calculations of the body weight multiplier translated the resultant force of 3774.39N to 3.11, at the toe propulsion stance in A3.

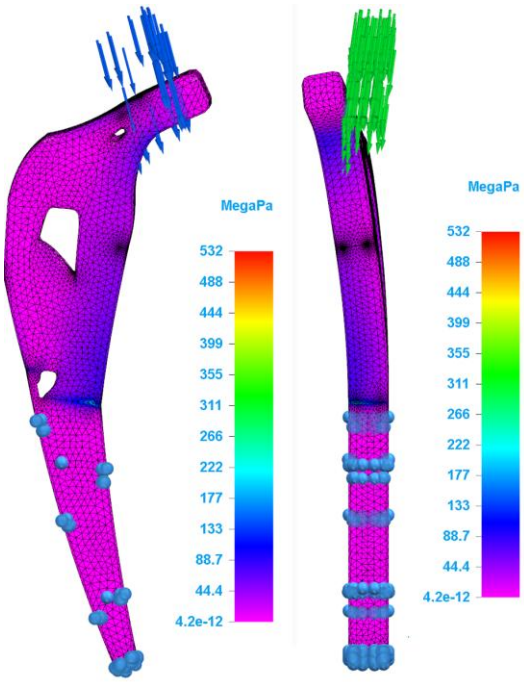

Figure 5.2 Stress concentration zone and yield stress in Scenario A3

Impact and Load Transfer – Matrices B&C Simulation (For H7R & H4L)

The vertical impact with the acceleration which is distributed on multi axial loads represents a biomechanical challenge, introduced in the ascending and descending stairs simulation.

The initial step up phase of scenario B1 has generated a sudden impact with a body weight multiplier amount of 2.50, with the localized stress maximum being 241, translating to 3.44 factor of safety. Although the resultant force was 2254.14 N, but the body weight multiplier is lower than the impact of level walking due to the difference of the weight between the selected patient data set.

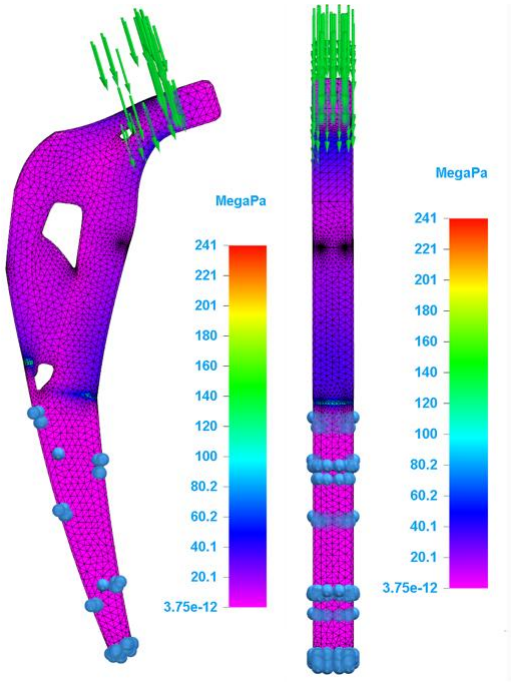

Figure 5.3 Stress concentration zone and yield stress in Scenario B1

However, during the peak of Matrix C simulation the scenario C2 body weight multiplier is only 1.46, during the phase of load transfer. it is only interesting to see the fact that the model has deformed in specific shape, which can translate the movement and the multi axial load distribution.

Fatigue and Cyclic Viability

In order to understand the specific criteria that determined the range of safety for the selection of factor safety 1.5 to 2.0, it is important to compare the maximum recording stress with the dynamic activity in order to evaluate the endurance limit of the selected material Ti-6Al-4V alloy.

Endurance limit is the maximum stress which is theoretically allowed to endure an infinite amount of cycle at without failing or sustaining fatigue, which in case of the titanium translates to 10 million cycles, if the load is within the 500-600 MPa.

The highest dynamic stress that was recorded in any of the tests that was performed over the dynamic analysis of the hip stem was 532 MPa, which means that the cyclical stress is significantly lower than the endurance limit of the medical grade titanium alloy, in order to conclude that the 25% mass reduced generative design prosthesis is not at risk of premature fatigue failure, however it's important to understand that the surface modeling is important in order to mitigate the stress concentration zones which can start micro fractures if the surface is not designed of organic curves. Theoretically the stem can withstand safe life span of the standard 15 to 20 years of requirement for the THA.

Dynamic FEA was conducted in order to ensure the long term survivability for the 25% reduced stem utilizing the calculated matrices from chapter 4 which maps with the telemetry data set of the selected (H9L, H7R and H4L) To simulate multi axial stresses of human locomotion daily activities.

5.1.3 Biomedical Validation

The biomedical viability is integrated as an approach that leverages the loading vectors from the telemetry dataset in order to create simulation for the generative algorithm that does not blindly but purposefully hollows the structure in order to imitate the density of the human cancellous bones. Therefore, the weight reduction of 25% is not an engineering efficiency metric, but it's a physiological upgrade that can help extend the lifespan, and improve the quality of life for the patient in long term.

Osseointegration

The generative geometry introduces advantages on the interface that solid stems does not necessarily apply, solid stems apply methods of coating and surface roughening in order to help the fixation, but the generative design can allow the bone to integrate with the structure, which means that after the implantation, the bone starts to fill the cavities in order to provide better stability against rotational stresses compared to the solid stem.

The long-term effect for generative design structures over the surface of the stem Is ideal as it promotes the vascularization and bone in growth.

Compliance with Wolff's Law to Mitigate Stress Shielding

As it was established in the literature review, the main failure mode of cementless THA is that the stem starts to loosen due to the highly stiff solid titanium stem contact with the bone, which is explained by the stress shielding phenomenon. Greater percentage of the mechanical strain is distributed over the surrounding bone in case of the generative design structures, which replaced the mismatch of the solid stem, meaning that theoretically; the restored mechanical stimulation can promote

the forming cells to maintain the bone density in order to avoid the implant loosening at late stages.

5.2 Comparative Manufacturing Assessment

In the assessment for the comparative analysis in cases of CNC manufacturing and AM, it is important to realize all the aspects of the manufacturing from the beginning of the life cycle of the product, to the cost analysis. For powder bed fusion in SLS/SLM manufacturing, and in order to prepare a better comprehensive analysis for the cost of manufacturing, it is important to realize the waste from the material and the consumption of energy, as well as the amount of time needed to design the product, manufacture it, and prepare for usage in surgeries.

The selection for the titanium alloy Ti-6Al-4V is also compatible with the advanced manufacturing technique that relies on Powder Bed Fusion (PBF) like the SLM manufacturing technology, the effective Integration of porous surfaces lattice structure is also possible with the titanium stem which can further reduce the stiffness of the system in order to perfectly align with the bone tissues, which maximizes the clinical viability and Promotes osseointegration.

5.2.1 Digital Data Foundation & Production Economics

In order to evaluate the feasibility of mass production for the mass customised hip implant, the study will be assessed on a lot size of 20 pieces, in order to evaluate the production cost from the aspects of material, energy, machine operating costs, and finishing for the standard 5-axis CNC machine on the solid model, and the direct metal laser sintering EOS M290 for the optimised generative designed hip implant.

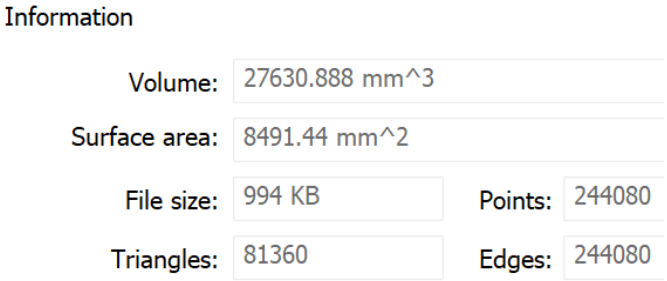

Figure 5.4 Volume and Geometric Information

With a selection of the 0.001 conversion tolerance the algorithm has produced the complex mesh of 81,360 triangles for the generative algorithm which means that exported file is large, but it's necessary 4 the required tolerances in the engineering of medical field applications, 244,080 points and edges or included in

the data set, which means that the measurement of the tool path, and processing time for the production is calculated accordingly.

Table 5.1 Analysis of CNC and AM.

Comparison Aspect	**SM (5-axis CNC) Mass Produced**	**AM (DSLM) Mass customized**
Process type	Removes material from blank (Subtractive)	From metal powder builds parts layer by layer (Additive)
Material waste (Complex parts)	Less total waste than optimized AM; solid has simpler geometry	Optimized waste ≈ 60.2% higher than CNC despite similar input due to Support Structure Forms
Part weight	Not optimized (100%)	Optimized ≈ 25% less than CNC
Geometry complexity	Limited internal channels	Complex internal features: inner channel structures
Post-processing	Surface finishing, coating	Powder removal, CNC finishing
Energy per part consumption	Higher specific energy: 5kWh (idle) to15 kWh = €84	Lower specific energy: 1.5 kWh (idle) to 5.5 kWh = €56
Pre-Production	€60 (€3/piece)	€3600 (€180/piece)
Material cost	€614	€807
Production volume	20 parts	20 parts
Logistics	€100	€300
Overhead and operating costs	€1400	€2500
Batch total cost	€2428 (€121.40 /unit)	€8363 (€418.15/unit)

Assuming that the cost for the engineering reproduction time is identical for the 20 solid stems, with the engineering rate of €60 per hour, makes the cost of Pre-Production in CNC at €60, and €3600 for the AM in consideration that mass customization requires a minimum of 3 hours per unit.

Electricity Rate is at €0.15/kWh, 28 hours for CNC, and 83 hours for AM.

Logistics is at €15/part in AM and €10/part in CNC.

5.2.2 Additive Manufacturing Assessment (EOS M290 DMLS)

In the parameter selection for the additive manufacturing assessment the digital resolution which is the tolerance for the conversation has been set to 0.001, which means that algorithm that determines the path of the fracturing using the layers as flat surfaces, when it starts to create the surfaces, the digital surface which is one that was designed without considering the mesh, has the potential to only deviate a maximum of 1 x 10^{-6}m, the With the only downside of using the lower conversion rate; is that the file that is created as an STL file is larger; due to the large amount of data stored.

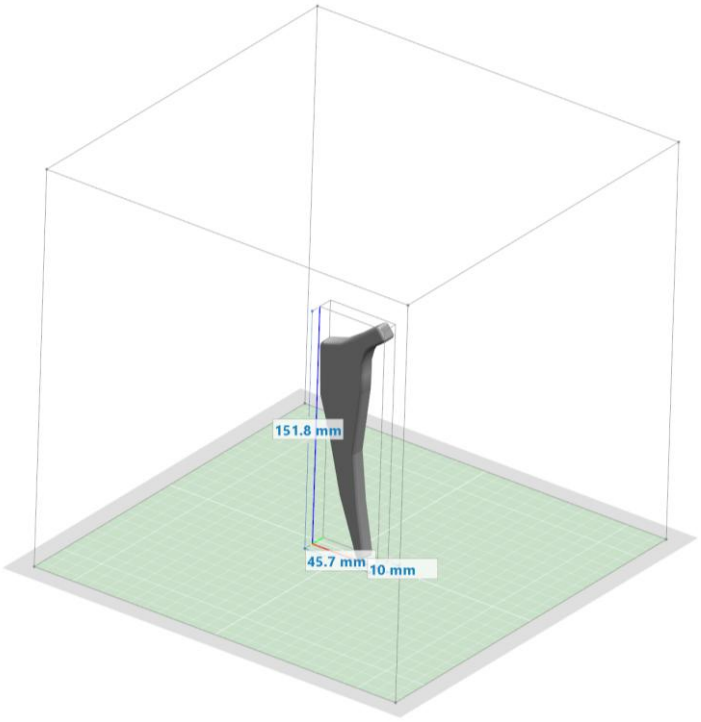

Figures 5.5. 3D Printing Assessment Setup

Current evaluation is directly related to the original model for the 3D printing, which are analyzed regardless of the manufacturing technology, as if it was FDM SLA, SLS or SLM. The data in the information table shows that the model has 81,360 triangles, which means that there are approximately 10 triangles in every millimeter of this part, giving the model exceptionally high resolution while providing fine finished surface to use it in the medical application field.

It is possible to build the generative designed stem vertically as the build volume of the EOSM 290 is 250x250x325 Is the maximum size of the hip stem is 151.8mm so that when it's oriented to utilize the Z height in order to reduce the support structures that are needed.

As assessed 244,080 Points, 244,080 Edges. Ratio: $244{,}080/81{,}360 = 3$.

Which translates directly to the angles of triangles are three times the number of triangles, meaning that the high fidelity of the model, did not conclude in any deviations in calculating the position of every corner simultaneously. The estimated production time for the EOS M290 is based on the build rate of approximately 8000 mm^3/hr Which means that the final volume of 27,630.9 mm^3 is approximately built with an exposure time of 3.45 hours.

5.2.3 Subtractive Manufacturing Assessment (5-Axis CNC)

CNC manufacturing has limited capabilities for creating Internal channels even in the most advanced machines of 5 axis, as well as the creation of nanostructures, or lattice structures, which translates to poor performance in advanced medical field applications. AM can provide the exact missing key points of CNC conventional manufacturing, but lacks the reliability, and there is still great amount of time that it takes to advance and be established, similarly to the current state of technology in CNC manufacturing.

The ultimate failure point in case of the CNC Assessment for the production of Generative Designed Hip stem, as it is physically unable to produce the complex internal network of channels and support structures, as well as the lack of organic cavities that are necessary in order to avoid the stress concentration zones that was discussed in the biomechanical validation of the current chapter, resulting in a bottleneck for the solution that can advance the practice of orthopedic engineering for the promotion of osseointegration and the vascularization.

Even with the current state of the art 5-axis CNC milling machines, it is impossible to produce convoluted cavities, which means that in order to account for the increased 8491.44 mm^2, it is an internal shadowed region that is physically impossible to be milled, therefore, the assessment for creating a subtractive manufactured Hip stem has no scientific ground to be carried on the generative designed hip stem.

Beyond the physical limitations of the cutting tool, the digital transformation for the design mesh, with the 0.001 mm conversion tolerance requires extensive post processing, as the CNC toolpath struggles to generate the non-prismatic organic surfaces, which ultimately rules out the option in case of the CNC subtractive manufacturing from the biomechanical point of view too.

6 Summery and Conclusion

The evolution for THA is directly driven by the imperative to reduce the complications after the operation specifically the stress shielding, which if only relying on the mechanical safety of the implants, produces stiffness mismatch with the surrounding bone tissues.

The primary objective of this thesis is to investigate and try to resolve this mismatch by integrating the topology optimization with a framework for validation that relied on empirical telemetry data. Feasibility assessment was also conducted in order to conclude the ultimate selection of the manufacturing technology as a superior production method for either mass produced or mass customised medical devices.

6.1 Notes on This Thesis Findings

Serious efforts of improving and implementing measures in order to reduce the risk of many downsides, hopefully additive manufacturing are on emphasis today. However, more emphasis must be put on the lifestyle of people involved at the risk of requiring the hip implant surgery. As it is always the ultimate solution, and the one that can last through generations.

Some discoveries and research work in Japan have already produced positive signs in implanting bone tissues in order to help recover removed damaged tissues, which can could be considered to have better integration in the human body, as the problem comes with all these implants even after performing the procedure, that the connection it has with the human body interface is not natural.

So the ultimate direction would always be to look for solutions that could integrate naturally, in any case of engineering decision, as it come to thinking that it is possible to create solutions without drawbacks, but in the circle of innovation, the bill is always due, if not for this time, but for the next generation, many reasons must be put into consideration in order to create a safe solution.

In the light of recent discoveries regarding the powder remnant inside the lattice structures that has been in additively manufactured implants, the remnants cause serious risk when not fully integrated with the part, or removed during the finishing process. It is safe to say that the conventional manufacturing technology still have

the limitations but produce solid results that can outperform any experimental technology until a huge amount of advancement has been put into place.

In case of medical field applications, It is important to note that the conventional manufacturing technologies may lack the advanced capabilities of the experimental technologies like additive manufacturing, although it is known that additive manufacturing has already been established to the point where it's capable of delivering on the promises of the technology being accessible to everyone, but it's still far from now.

So, in order to achieve the best results in case of medical application, it is possible to produce solid parts and then threading them by a very intricate drilling system in order to achieve the same results that can be achieved using the lattice structure which can only be producible by additive manufacturing in this case.

6.2 Contributions to Orthopaedic Engineering

The main contribution for the patient specific transition in the orthopaedic practise in this thesis is, that it provides a mathematical foundation for future design possibilities with the detailed economic assessment in order to bridge the gap between the mechanical theory and the logistics in medical applications. It is also important to organically shape the process in order to withstand extreme amount forces without localising yield.

6.3 Acknowledged Limitations in the Research

Boundary conditions that were applied in the FEA study were directly derived from the telemetry data set of patient profiles aged between 50 and 56, with variable weights, which means that in order to produce highly reliable data, it is necessary to study a wider demographic base.

The simulation assumed that the material exhibits isotropic properties, which means that in case of the titanium alloy that is produced in laser powder bed fusion machines, The results can exhibit variable properties of anisotropic mechanical behaviour depending on the build orientation and the toolpath

6.4 Future Work Direction

In future work direction, an approach of hybrid manufacturing workflows can be explored in order to create the modular pieces using the CNC machines, it is possible to introduce further advancements in the methodology in order to produce lattice structures, replacement using conventional technology, or trying to integrate machine learning models in order to reduce the computational needs that are the current bottleneck in these times of limited energy supply.

Acknowledgements

For the work of this thesis. It is important to give credits where it's due, to everyone who made this thesis work possible, and to every constructive advice that made this thesis note better. Thanks to Dr. Bodzás Sándor, my thesis supervisor, for his dedication in providing continuous guidance during the course of the thesis work, to Nemes Daniel for his advice on the methodology of the thesis work, to Dr. Mankovits Tamas for his constructive advice, and ultimately to my parents Abdullah and Fatima for the resources and support that they provided throughout the hard times and decisions during my academic career.

List of references/Bibliography

[1] Li H. [et al.]: Three-dimensional printing: The potential technology widely used in medical fields, In: *Journal of Biomedical Materials Research Part A*, 2020, 108(11), p. 2217–2229. DOI: 10.1002/jbm.a.36979.

[2] Cafolla D. [et al.]: 3D printing for feasibility check of mechanism design, In: *International Journal of Mechanics and Control*, 2016, 17(1), p. 3–12. ISSN 1590-8844.

[3] Alkhateib K. A. O.: Transmitting motion in mechanical assemblies using 3D printing technology, BSc Thesis, University of Debrecen, Faculty of Engineering, Debrecen, 2021, Nr: GT-BSC-OM 12/2022/2.

[4] Seabra M. [et al.]: Selective laser melting (SLM) and topology optimization for lighter aerospace components, In: *Procedia Structural Integrity*, 2016, 1, p. 289–296. DOI: 10.1016/j.prostr.2016.02.039.

[5] Rozvany, G. I. N.: "A critical review of established methods of structural topology optimization," In: *Structural and Multidisciplinary Optimization*, 37(3), 2009, pp. 217–237. DOI: 10.1007/s00158-007-0217-0.

[6] Szabó K.: Application of topological methods, In: *Design of Machines and Structures*, 2021, 11(1), p. 59–68. DOI: 10.32972/dms.2021.008.

[7] Du, J. & Olhoff, N.: Topological design of freely vibrating continuum structures for maximum values of single and multiple eigenfrequencies and frequency gaps, In: *Structural and Multidisciplinary Optimization*, 2007, 34, p. 91–110. DOI:10.1007/s00158-007-0101-y.

[8] Cleveland Clinic: Hip arthritis – patient education infographic, In: *Cleveland Clinic* {online} https://my.clevelandclinic.org/-/scassets/images/org/health/articles/hip-arthritis

[9] Silva J.: Comparative life cycle inventory of CNC machining and powder bed fusion Additive Manufacturing, MSc Thesis, Aalto University, School of Engineering, Programme in Mechanical Engineering – Product Development, 29.12.2022

[10] Kurtz S. [et al.]: Projections of primary and revision hip and knee arthroplasty in the United States from 2005 to 2030, In: *Journal of Bone and Joint Surgery – American Volume*, 2007, 89(4), p. 780–785. DOI: 10.2106/JBJS.F.00222.

[11] Orion Orthopedic Surgery: Total hip replacement surgery using direct anterior approach (DAA), In: Orion Orthopedic Surgery {online}

https://www.orionortho.sg/total-hip-replacement-using-direct-anterior-approach-daa (Accessed 02.11.2025).

[12] Dias J. M. [et al.]: Unveiling additively manufactured cellular structures in hip implants: a comprehensive review, In: *The International Journal of Advanced Manufacturing Technology*, 2023, 130(7), p. 1–50. DOI:10.1007/s00170-023-12769-0.

[13] Soliman, Md Mohiuddin [et al.]: A Review of Biomaterials and Associated Performance Metrics Analysis in Pre-Clinical Finite Element Model and in Implementation Stages for Total Hip Implant System, In: *Machine Learning Applications in Polymeric Biomaterials*, 2022, 14(20), p. 4308. https://doi.org/10.3390/polym14204308.

[14] Kocagoz S. B.: Crevice corrosion at the femoral head-stem interfaces in total hip arthroplasty, PhD Dissertation, Drexel University, Department of Biomedical Engineering, 2020.

[15] Xiao, Zhongmin [et al.]: Multi-Scale Topology Optimization of Femoral Stem Structure Subject to Stress Shielding Reduce, In: *Materials*, 2023, 16(8), p. 3151. https://doi.org/10.3390/ma16083151.

[16] Hip implant 3D CAD model (femoral stem and acetabular cup assembly), In: *GrabCAD Model Library* {online} https://grabcad.com/library/hip-implant-17 (Accessed 11.06.2025)

[17] Naghavi, Seyed Ataollah [et al.]: Stress Shielding and Bone Resorption of Press-Fit Polyether–Ether–Ketone (PEEK) Hip Prosthesis: A Sawbone Model Study, In: *Polymers*, 2022, 14(21), p. 4600. https://doi.org/10.3390/polym14214600.

[18] Tan, Nathanael, van Arkel, Richard J.: Topology Optimisation for Compliant Hip Implant Design and Reduced Strain Shielding, In: *Materials*, 2021, 14(23), p. 7184. https://doi.org/10.3390/ma14237184.

[19] Namvar, A. [et al.]: Finite element analysis of patient-specific additive-manufactured implants, In: *Frontiers in Bioengineering and Biotechnology*, 2024, 12, p. 1386816. https://doi.org/10.3389/fbioe.2024.1386816.

[20] Boyle, C.: Computational Study of Wolff's Law Utilizing Design Space Topology Optimization: A New Method for Hip Prosthesis Design, MSc Thesis, Queen's University, Mechanical and Materials Engineering, 2010.

[21] Kovács Á. É. [et al.]: Comparative Analysis of Bone Ingrowth in 3D-Printed Titanium Lattice Structures with Different Patterns, In: *Materials*, 2023, 16(10), 3861. DOI: 10.3390/ma16103861.

[22] Guo, Liyao [et al.]: On the design evolution of hip implants: A review, In: Materials & Design, 2022, 216, p. 110552. ISSN 0264-1275. https://doi.org/10.1016/j.matdes.2022.110552.

[23] Alkentar, R., & Mankovits, T.: Development of patient-specific lattice structured femoral stems using finite element analysis and machine learning. *Crystals*, 2025, 15(7), 650. DOI: 10.3390/cryst15070650.

[24] [9] Ghosh, Rajdeep – Chanda, Souptick – Chakraborty, Debabrata: Application of finite element analysis to tissue differentiation and bone remodelling approaches and their use in design optimization of orthopaedic implants: A review, In: *International Journal for Numerical Methods in Biomedical Engineering*, 2022, 38(10), p. e3637. https://doi.org/10.1002/cnm.3637

[25] Alkentar, R., & Mankovits, T.: Development of surrogate model for patient-specific lattice-structured hip implant design via finite element analysis. *Crystals*, 2023, 13(7), 3522. DOI: 10.3390/cryst13010113.

[26] Alkentar, R., & Mankovits, T.: Optimization of additively manufactured and lattice-structured hip implants using the linear regression algorithm from the Scikit-Learn library. *Applied Sciences,* 2023*,* 13(10), 5451. https://doi.org/10.3390/app12115451.

[27] Bergmann, Georg [et al.]: Standardized Loads Acting in Hip Implants, In: PLoS One, 2016, 11(5), p. e0155612. https://doi.org/10.1371/journal.pone.0155612.